INSTITUTO
DE FÍSICA

preprint

IFUSP/P-239

ISING MODEL WITH COMPETING AXIAL INTERACTIONS IN THE PRESENCE OF A FIELD

by

C.S.O. Yokoi* , M.D. Coutinho-Filho† ,
and S.R. Salinas*

* Instituto de Física, Universidade de São Paulo, C.P. 20.516, São Paulo, SP, Brazil

† Departamento de Física, Universidade Federal de Pernambuco, 50.000 Recife, Pe., Brazil

UNIVERSIDADE DE SÃO PAULO
INSTITUTO DE FÍSICA
Caixa Postal - 20.516
Cidade Universitária
São Paulo - BRASIL

ISING MODEL WITH COMPETING AXIAL INTERACTIONS IN THE PRESENCE OF A FIELD

by

C.S.O. Yokoi* , M.D. Coutinho-Filho† , and S.R. Salinas*

* Instituto de Física, Universidade de São Paulo, C. P. 20.516, São Paulo, SP, Brazil

† Departamento de Física, Universidade Federal de Pernambuco, 50.000 Recife, Pe., Brazil

Sept/80

ABSTRACT

We study a layered Ising model with competing interactions between nearest and next-nearest layers in the presence of a magnetic field. The analysis is carried out in the mean-field approximation with one effective field for each layer. The high-temperature region is studied analytically. The λ-surface, separating the paramagnetic and the modulated phases, is bounded by two-lines of tricritical points which join smoothly at the Lifshitz point and terminate at multi-critical points, beyond which lines of critical and bicritical endpoints are expected to appear. The magnetization structure near the λ-surface can be described as having an almost sinusoidal oscillation, with the higher harmonic components contributing as perturbations. Both odd and even higher harmonic components are present in non-zero fields, and the n-th harmonic component depends asymptotically on the n-th power of the main harmonic component. The low-temperature region is studied numerically. We construct T-H phase diagrams, which exhibit a variety of modulated phases, for various values of the ratio of the strength of the competing interactions. Numerical evidence of the devil's staircase behavior is found either as a function of temperature or applied magnetic field.

I. INTRODUCTION

Considerable attention has in recent years been devoted to the investigation of systems displaying modulated ordered phases. Two aspects of these systems have particularly attracted the attention of several workers. First, the proposal of a new multicritical point, the so-called Lifshitz point[1], which divides the phase diagram into modulated, disordered and uniformly ordered phases. Second, the renewed interest in commensurate and incommensurate structures[2], which occur in modulated phases, together with the problem of the phase transitions associated with these structures.

An Ising model on a simple cubic lattice with nearest neighbor ferromagnetic couplings, and next-nearest neighbor competing antiferromagnetic couplings in a direction parallel to a single lattice axis, is probably the simplest magnetic spin model displaying a Lifshitz point and a complex modulated phase. For this reason, although having been proposed many years ago[3], this model has been the object of quite a substantial amount of theoretical work in the last few years. The vicinity of the Lifshitz point and the high temperature region of the phase diagram in the T-p plane, where T is the absolute temperature and p is the ratio of competing exchange interactions, have been studied by renormalization group[1,4], high-temperature series expansions[5] and Monte Carlo techniques[6]. On the other hand, Monte Carlo calculations[7], low-temperature series expansions[8], mean-field calculations and soliton theory[9] were used to study the low

temperature modulated region. From the experimental side, it is appropriate to stress the physical relevance of this simple model. For instance, since the early sixties similar models have been widely used to explain the sinusoidal ordering of some rare earth metals such as erbium[3]. More recently, the complex succession of commensurate phases of CeSb as a function of temperature[10] has been qualitatively explained on the basis of a closely related model[11]. Also, it has very recently been indicated[12], by measurements of the transverse differential susceptibility in MnP , that this material displays a uniaxial Lifshitz point belonging to the same universality class as the model considered here.

In this paper we study, within the mean-field approximation, the behavior of the above-mentioned Ising model in the presence of an applied magnetic field. Our motivation for this study was the well known fact that the magnetic field may change the nature of phase transitions in a fundamental way, inducing the appearence of multicritical points, such as tricritical points in metamagnetic systems[13]. Also, the response of various modulated phases to the applied field, and the field dependence of the phase diagrams, is a matter of intrinsic interest. Apart from these motivations, we believe that from the experimental point of view magnetic fields play a very important role. For instance, finer details of the modulated phases, e.g., the devil's staircase behavior[11] , could be sought as a function of the applied magnetic field, and we hope that a theoretical guidance, even though in a mean-field approximation, will be useful.

The layout of this paper is as follows: In Sec. II a precise definition of the model is given and relevant expressions in the layer-by-layer mean-field approximation are derived. Some calculations in zero field are briefly presented in Sec. III. In particular, expressions for the λ-lines and the Lifshitz point, and an asymptotic expression for the first-order transition line are obtained. The effects of the higher harmonic components of the magnetization near the modulated-paramagnetic transition are discussed. In Sec. IV, devoted to the mean-field calculations in the presence of an applied field, the expressions for the λ-surface and the lines of tricritical points are determined. Higher harmonic components of the magnetization are calculated and their effect on the location of tricritical points is taken into account. The stability of the tricritical points is investigated in Sec. V within the framework of the Landau theory of phase transitions. In Sec. VI, results of the numerical calculations in the modulated phase are presented, and the main features of the effect of an applied field on the various commensurate structures are examined. In Appendix A the mean-field solutions of the model in zero field are compared to the phenomenological Landau expansion, and the influence of umklapp terms on the commensurate phases is discussed. The ground state of the model is discussed in Appendix B. In Appendix C the spherical version of the model is studied, and it is shown that in this case no tricritical behavior occurs. Finally, some conclusions are presented in Sec. VII.

II. MEAN-FIELD EQUATIONS

We consider a spin-1/2 Ising model on a simple cubic lattice with exchange interactions J_o between nearest neighbors in the xy plane, and competing interactions J_1 and J_2 between first and second neighbors respectively along the z direction (see Fig. 1). In the presence of an applied field H the Hamiltonian may be written as

$$\mathcal{H} = -\frac{1}{2} \sum_{x,y,z} \left\{ J_o \; \sigma_{x,y,z} \; \sigma_{x\pm1,y\pm1,z} + J_1 \; \sigma_{x,y,z} \; \sigma_{x,y,z\pm1} + J_2 \; \sigma_{x,y,z} \; \sigma_{x,y,z\pm2} \right\} - \sum_{x,y,z} H \; \sigma_{x,y,z} \quad , \tag{II.1}$$

where we take the lattice spacing equal to unit, and the sums are over all lattice sites. For definiteness we assume periodic boundary conditions, with period N, along the three directions.

The mean-field expression for the Gibbs free-energy $G(T,H,N)$ of this system may be derived via the Bogoliubov inequality[14]

$$G \leq \Phi = G_o + \langle \mathcal{H} - \mathcal{H}_o \rangle_o \quad , \tag{II.2}$$

where

$$G_o = -kT \, \ell n \left\{ \sum_{\{\sigma\}} \exp(-\beta \mathcal{H}_o) \right\} \quad , \tag{II.3}$$

$\beta = 1/kT$, $\mathcal{H}_o$ is any trial Hamiltonian, the sum is over spin configurations, and the average $\langle \mathcal{H} - \mathcal{H}_o \rangle_o$ is taken with respect to $\mathcal{H}_o$. In order to obtain the mean-field approximation, we consider the free trial Hamiltonian

$$\mathcal{H}_o = - \sum_{x,y,z} \eta_z \, \sigma_{x,y,z} \quad , \tag{II.4}$$

where η_z is a variational parameter associated with the layer z . With this choice of $\mathcal{H}_o$ we have

$$\Phi = - kT \, N^2 \sum_z \ell n \left[2 \cosh \beta \eta_z \right] -$$

$$- \frac{1}{2} N^2 \sum_z \left[4J_o \, m_z^2 + J_1 \, m_z (m_{z-1} + m_{z+1}) + J_2 \, m_z (m_{z-2} + m_{z+2}) \right] +$$

$$+ N^2 \sum_z (\eta_z - H) \, m_z \quad , \tag{II.5}$$

where the function m_z , that is, the average magnetization per spin in layer z , is given by

$$m_z = \tanh \beta \eta_z \quad . \tag{II.6}$$

The mean-field approximation is obtained by minimizing the right-hand side of Eq. (II.2) with respect to the variational parameters η_z . Therefore, the mean-field Gibbs free-energy is

$$G_{MF} \, (T,H,N) = \Phi \quad , \tag{II.7}$$

with the parameters η_z given by

$$\eta_z = H + 4J_o\, m_z + J_1(m_{z-1} + m_{z+1}) + J_2(m_{z-2} + m_{z+2}) \quad . \qquad (II.8)$$

Substituting Eqs. (II.6) and (II.8) into Eq. (II.5) we may write the mean-field Gibbs free-energy in the form

$$N^{-3} G_{MF}(T,H,N;\{m_z\}) = - kT\, \ell n\, 2 + \frac{kT}{2N} \sum_z \{(1+m_z)$$

$$\ell n(1+m_z) + (1-m_z)\, \ell n\, (1-m_z)\} - \frac{1}{2N} \sum_z \{4J_o\, m_z^2 +$$

$$+ J_1\, m_z(m_{z-1} + m_{z+1}) + J_2\, m_z(m_{z-2} + m_{z+2})\} - \frac{H}{N} \sum_z m_z \,, \qquad (II.9)$$

where m_z is given by the solution of the system of N coupled equations

$$m_z = \tanh \beta \left[H + 4J_o\, m_z + J_1(m_{z-1} + m_{z+1}) + \right.$$

$$\left. + J_2(m_{z-2} + m_{z+2})\right] \quad . \qquad (II.10)$$

It should be remarked that this set of equations admits, in general, more than one solution. In this case a physically relevant solution must be found which gives the lowest value for the mean-field Gibbs free-energy (II.9).

III. MEAN-FIELD CALCULATIONS IN ZERO FIELD

For the sake of completeness, and to emphasize some aspects of our calculations, we present in this chapter a few results in zero field, some of which have been obtained by a number of authors. It is well known that the model system may undergo a second order phase transition from a paramagnetic to a sinusoidally ordered phase with varying periodicity. For finite N the values of the wave vector q are limited to the multiples of $2\pi/N$ due to the periodic boundary conditions. To allow for commensurate as well as incommensurate periodicities, we must take the thermodynamic limit $N \to \infty$. In this case, which will be considered in our work unless otherwise stated, the wave vectors vary continuously in the first Brillouin zone.

A. The order-disorder transition lines.

The transition between the disordered ($m_z = 0$) and the ordered ($m_z \neq 0$) phases can be determined very simply from Eq. (II.10). For small m_z we have

$$m_z \simeq \beta \left[4J_o \, m_z + J_1(m_{z-1} + m_{z+1}) + J_2(m_{z-2} + m_{z+2}) \right] . \qquad \text{(III.1)}$$

If we introduce the Fourier components of m_z, according to

$$m_z = \sum_q m_q \, e^{iqz} , \qquad \text{(III.2)}$$

where the sum is over the first Brillouin zone $(-\pi < q \leq \pi)$,

Eq. (III.1) yields

$$m_q \approx \beta J(q)\, m_q \quad , \tag{III.3}$$

where

$$J(q) = 4J_o + 2J_1 \cos q + 2J_2 \cos 2q \quad . \tag{III.4}$$

As we decrease the temperature of the system, Eq. (III.3) will begin to exhibit non-vanishing solutions for a critical value of q which maximizes $J(q)$. Thus, the transition temperature is determined by

$$kT_c = \max_q \{J(q)\} = J(q_c) \quad . \tag{III.5}$$

The ordered phases just below the transition temperature are shown in the diagram of Fig. 2. The modulated phase near the transition temperature is characterized by the wave vector q_c given by

$$\cos q_c = - J_1/4J_2 \quad , \tag{III.6}$$

whereas $q_c = 0$ in the ferromagnetic phase and $q_c = \pi$ in the metamagnetic phase.

In this work we consider mainly the case $J_o, J_1 > 0$ and $J_2 < 0$. The expressions for the transition lines from the disordered to the ordered phases in the T-p plane (see Fig. 3), where $p = -J_2/J_1$, follow immediately from Eq. (III.5). The field parameter p measures the competition

between nearest and next-nearest spins in the z direction. For $p < 1/4$ the system orders ferromagnetically, and the paramagnetic-ferromagnetic λ-line is given by

$$kT_o = J(0) = 4J_o + 2J_1 + 2J_2 = 4J_o + \frac{3}{2} J_1 - 2J_1 \Delta p \quad , \qquad (III.7)$$

where $\Delta p = p - 1/4$. For $p > 1/4$, the system orders sinusoidally, and the paramagnetic-sinusoidal λ-line is given by

$$kT_\lambda = J(q_c) = 4J_o - 2J_2 - \frac{J_1^2}{4J_2} = kT_o + 16J_1 \Delta p^2 + O(\Delta p^3) \quad . \qquad (III.8)$$

It then follows that both λ-lines join smoothly at the Lifshitz point (T_L, p_L) where $p_L = 1/4$ and

$$kT_L = 4J_o + \frac{3J_1}{2} \quad . \qquad (III.9)$$

In order to obtain an asymptotic expression, close to the Lifshitz point, for the ferromagnetic-modulated transition line, and to examine the nature of this transition, we have to go beyond Eq. (III.1) and consider the higher harmonic components of the magnetization per layer. This will be done in the next paragraph.

B. Higher harmonic components of the magnetization.

The mean-field values of the magnetization per spin in a layer are given by the solutions of the set of coupled equations (II.10). Near the transition m_z is small, and we may write the following expansion,

$$\beta \left[4J_o\, m_z + J_1(m_{z-1} + m_{z+1}) + J_2(m_{z-2} + m_{z+2})\right] =$$

$$= \tanh^{-1} m_z = m_z + \frac{1}{3} m_z^3 + \frac{1}{5} m_z^5 + \ldots \quad . \qquad \text{(III.10)}$$

A purely sinusoidal magnetization

$$m_z = M_1 \cos(q_c z + \phi_1) \qquad \text{(III.11)}$$

is clearly inconsistent with Eq. (III.10). Therefore, we will seek a solution in the form of a Fourier series

$$m_z = M_1 \cos(q_c z + \phi_1) + M_3 \cos(3q_c z + \phi_3) +$$

$$+ M_5 \cos(5q_c z + \phi_5) + \ldots \qquad \text{(III.12)}$$

where, in this particular case, we need not consider the even harmonic components. Also, the coefficients M_n are, for convenience, supposed real. Substituting Eq. (III.12) into Eq. (III.10), and comparing the coefficients of the same harmonics, we obtain in leading order

$$M_1 \approx \pm 2 \left(1 - \frac{T}{T_c}\right)^{1/2} , \qquad \text{(III.13)}$$

$$M_3 \approx \frac{-1}{12} \left[1 - \frac{J(3q_c)}{J(q_c)}\right]^{-1} M_1^3 , \qquad \text{(III.14)}$$

$$M_5 \approx \frac{1}{240} \left[1 - \frac{J(5q_c)}{J(q_c)}\right]^{-1} \left\{5 \left[1 - \frac{J(3q_c)}{J(q_c)}\right]^{-1} - 3\right\} M_1^5 \quad . \qquad \text{(III.15)}$$

In general, the coefficient of the n-th harmonic term, where n is an odd integer, approaches T_c as $(T_c - T)^{n/2}$. One of the phases, say ϕ_1, is arbitrary, but then the other phases are determined by the condition

$$\phi_n = n\,\phi_1 + \nu\,\pi \qquad \text{(III.16)}$$

where ν is an integer. Expressions (III.13) to (III.15) correspond to the choice $\nu = 0$. Strictly speaking, the phase ϕ_1 is fully arbitrary only for incommensurate wave vectors. For commensurate wave vectors the expansion (III.12) is finite and the phase ϕ_1 has to be chosen properly in order to minimize the free-energy. This point is discussed in more detail in Appendix A.

Close to the λ-line, our results show that the modulated phase is fairly well represented by a sinusoidal layer magnetization with wave vector q_c. The higher harmonic components contribute as perturbations, and become more important as we penetrate into the modulated region.

C. The first-order transition line.

In zero field the Gibbs free-energy may be expanded as the following power series in m_z,

$$N^{-3} G_{MF}(T,H=0,N;\{m_z\}) = -\,kT\,\ell n\,2 + \frac{1}{2N}\sum_z \Big\{ -\Big[4J_o\, m_z^2 + J_1\, m_z (m_{z-1} + m_{z+1}) + J_2\, m_z (m_{z-2} + m_{z+2}) \Big] + kT\, m_z^2 + \frac{1}{6}\,kT\, m_z^4 + \frac{1}{15}\,kT\, m_z^6 + \ldots \Big\} \quad . \qquad \text{(III-17)}$$

Decomposing m_z in its Fourier components as in expression (III.12), we may also write

$$N^{-3} G_{MF} = - kT \ \ell n \ 2 + \frac{1}{4} \left[kT - J(q_c) \right] M_1^2 +$$

$$+ \frac{1}{4} \left[kT - J(3q_c) \right] M_3^2 + \frac{1}{32} kT \ (M_1^4 +$$

$$+ \frac{4}{3} M_1^3 \ M_3) + \frac{1}{96} kT \ M_1^6 + \ldots \quad . \qquad \text{(III.18)}$$

Since M_1 is of order $(T_c - T)^{1/2}$, and M_3 of order M_1^3, we need not consider the third harmonic component in the leading asymptotic expression of the free-energy, which is given by

$$N^{-3} G_{MF}^{(m)} \approx - kT \ \ell n \ 2 - \frac{1}{2} kT \ (1 - \frac{T}{T_\lambda})^2 \quad . \qquad \text{(III.19)}$$

To obtain an expression for the Gibbs free-energy in the ferromagnetic phase, we have to go back to Eq. (III.17) and make $m_z = m$ for all z. In this way we have

$$N^{-3} G_{MF} = - kT \ \ell n \ 2 - \frac{1}{2} J(0) \ m^2 + \frac{kT}{2} \left[m^2 + \frac{1}{6} m^4 + \ldots \right] \ , \qquad \text{(III.20)}$$

and in leading order

$$m \approx \pm \sqrt{3} \ (1 - \frac{T}{T_o})^{1/2} \quad . \qquad \text{(III.21)}$$

The leading asymptotic expression for the free-energy in the

ferromagnetic phase is thus given by

$$N^{-3} G_{MF}^{(f)} \approx - kT \ln 2 - \frac{3}{4} kT \left(1 - \frac{T}{T_o}\right)^2 \quad . \qquad \text{(III.22)}$$

Equating the free-energies (III.19) and (III.22) we obtain the following asymptotic expression for the ferromagnetic-modulated transition line close to the Lifshitz point

$$kT_1 \approx kT_o - (2 + \sqrt{6})\ 16\ J_1\ \Delta p^2 \quad , \qquad \text{(III.23)}$$

where T_o is defined by Eq. (III.7). This is a line of first-order transitions, with a jump of the entropy given asymptotically by

$$N^{-3}(S^{(m)} - S^{(f)}) \approx 8\sqrt{6}\ \frac{J_1}{T_1}\ \Delta p^2 . \qquad \text{(III.24)}$$

The three transition lines T_o , T_λ and T_1 join with a common tangent at the Lifshitz point, as depicted in Fig. 3.

Since it has recently been argued, on the basis of Monte Carlo calculations[7,15], that the ferromagnetic-modulated transition line might be of second order near the Lifshitz point, it is worth emphasizing the first order nature given by our mean-field results. Also, it is worth to remark that the higher harmonic components have no influence either on the critical lines (T_o and T_λ) for $H = 0$, or on the first-order ferro-modulated transition line T_1 asymptotically close to the Lifshitz point. However, not only is T_1 affected

by the higher harmonic components when we are sufficiently far from T_L, but, more significantly, the nature of the transitions may change in the presence of a magnetic field and the higher harmonic components have to be properly considered. This will be the main point of the next chapter.

IV. MEAN-FIELD CALCULATIONS IN NON-ZERO FIELDS

A. The order-disorder transition surface.

In the presence of a magnetic field, Eq. (II.10) admits a non-vanishing uniform solution $m_o = m_z$, for all z, which is determined by

$$m_o = \tanh \beta \left[H + J(0)\, m_o \right] \quad . \tag{IV.1}$$

At high temperatures this solution gives the lowest free-energy, that is, the system is in the paramagnetic phase. As the temperature is decreased, however, a nonuniform solution may emerge with lower free-energy. In the modulated phase and close to the transition we may write

$$m_z = m_o + \delta m_z \quad , \tag{IV.2}$$

where δm_z goes to zero as one approaches the critical surface. Substituting this expression for m_z into Eq. (II.10) we obtain

$$\beta \left\{ 4J_o \, \delta m_z + J_1 (\delta m_{z-1} + \delta m_{z+1}) + J_2 (\delta m_{z-2} + \delta m_{z+2}) \right\} =$$

$$= \frac{1}{1-m_o^2} \, \delta m_z + \frac{m_o}{(1-m_o^2)^2} \, \delta m_z^2 + \frac{1+3m_o^2}{3(1-m_o^2)^3} \, \delta m_z^3 + \ldots \qquad \text{(IV.3)}$$

Now δm_z can be expanded in a Fourier series,

$$\delta m_z = \sum_q m_q \, e^{iqz} \quad , \qquad \text{(IV.4)}$$

so that Eq. (IV.3) gives in first order

$$m_q = \beta (1 - m_o^2) \, J(q) \, m_q \quad , \qquad \text{(IV.5)}$$

which is analogous to Eq. (III.3) of the last chapter. The critical surface is thus given by

$$\frac{kT}{1-m_o^2} = \max_q J(q) = J(q_c) \quad , \qquad \text{(IV.6)}$$

where m_o is related to H by Eq. (IV.1). Eq. (IV.6) shows that the periodicity of the modulated phase close to the critical surface is a function of the parameter p only, that is, it does not depend either on T or on H. For small fields, we may write the equation for the critical surface in the form

$$\frac{kT}{J(q_c)} \approx 1 - \frac{H^2}{\left[J(q_c) - J(0) \right]^2} \quad , \qquad \text{(IV.7)}$$

which shows the usual quadratic depression of the critical temperature by the applied field.

B. Higher harmonic components of the magnetization

As it was shown in the last paragraph, close to the critical surface δm_z is determined by Eq. (IV.3). The solution of this equation can be sought in the form of a Fourier expansion

$$\delta m_z = M_o + M_1 \cos(q_c z + \phi_1) + M_2 \cos(2q_c z + \phi_2) +$$

$$+ M_3 \cos(3q_c z + \phi_3) + \ldots \quad , \qquad \text{(IV.8)}$$

where the even harmonic components should be duly taken into account. For convenience we will assume that $M_o, M_1, M_2, \ldots$ are real numbers. Substituting expansion (IV.8) into Eq. (IV.3), and comparing the coefficients of the same harmonics, we obtain in leading order

$$M_o \approx -\frac{1}{2} \frac{m_o \beta J(q_c)}{1 - \frac{J(0)}{J(q_c)}} M_1^2 \qquad \text{(IV.9)}$$

$$M_2 \approx -\frac{1}{2} \frac{m_o \beta J(q_c)}{1 - \frac{J(2q_c)}{J(q_c)}} M_1^2 \qquad \text{(IV.10)}$$

$$M_3 \approx \frac{-1}{12}\left[\beta\, J(q_c)\right]^2 \left[1 - \frac{J(3q_c)}{J(q_c)}\right]^{-1} \left\{(1 + 3m_o^2) - \right.$$

$$\left. - 6m_o^2 \left[1 - \frac{J(2q_c)}{J(q_c)}\right]^{-1}\right\} M_1^3 \quad , \qquad \text{(IV.11)}$$

and

$$M_1 \approx \pm 2\left[\beta\, J(q_c)\right]^{-1} \left\{1 - 3m_o^2 - 2m_o^2 \left[\frac{2J(0)}{J(q_c) - J(0)} + \right.\right.$$

$$\left.\left. + \frac{J(2q_c)}{J(q_c) - J(2q_c)}\right\}^{-1/2} \left[(1-m_o^2)\,\beta J(q_c) - 1\right]^{1/2} . \qquad \text{(IV.12)}$$

In general the n-th harmonic coefficient M_n, for $n \geq 2$, depends asymptotically on the n-th power of M_1. According to the discussion of the last section, the phase ϕ_1 is arbitrary, but the other phases are given by $\phi_n = n\phi_1$.

C. The line of tricritical points

In the previous paragraphs we have assumed that the transition is always continuous. However, it may become first order for high values of the applied field and low temperatures. To examine this possibility let us consider the total magnetization

$$M_T = \sum_{xyz} m_z = \sum_{xyz} (m_o + \delta m_z) \quad . \qquad \text{(IV.13)}$$

In the paramagnetic phase $\delta m_z = 0$ and we have simply

$$M_{T,p} = N^3 m_o \quad , \tag{IV.14}$$

whereas in the modulated phase δm_z is given by the Fourier expansion (IV.8), so that

$$M_{T,m} = N^3 (m_o + M_o) \quad . \tag{IV.15}$$

Eq. (IV.9) shows that m_o and M_o have opposite signs close to the transition surface. Accordingly, at fixed T, the total magnetization of the system is always smaller in the modulated phase than in the paramagnetic phase. Both branches of the total magnetization, in the M_T-H plane, meet with different slopes at the transition point. A loop of van der Waals, which characterizes the first order transitions, occurs when the derivative $(\partial M_{T,m}/\partial H)$ calculated at the transition point becomes negative. Therefore, the tricritical points are located by the condition

$$\left(\frac{\partial M_{T,m}}{\partial H}\right)_{\substack{\text{critical} \\ \text{surface}}} = \infty \quad . \tag{IV.16}$$

From equations (IV.9), (IV.12) and (IV.15) we obtain the following expressions for the tricritical temperature and field,

$$\frac{kT_{tr}}{J(q_c)} = 1 - \left\{3 + 2\left[\frac{2J(0)}{J(q_c) - J(0)} + \frac{J(2q_c)}{J(q_c) - J(2q_c)}\right]\right\}^{-1} \quad , \tag{IV.17}$$

$$\pm H_{tr} = - J(0) \left[1 - \frac{kT_{tr}}{J(q_c)}\right]^{1/2} + \frac{1}{2} k T_{tr} \ell n \frac{1 + \left[1 - \frac{kT_{tr}}{J(q_c)}\right]^{1/2}}{1 - \left[1 - \frac{kT_{tr}}{J(q_c)}\right]^{1/2}} \quad . \quad (IV.18)$$

In the vicinity of the Lifshitz point we may write

$$kT_{tr} \approx kT_o + \frac{232}{19} J_1 \Delta p^2 \quad , \quad (IV.19)$$

and

$$\pm H_{tr} \approx \frac{232}{19} \left(\frac{72}{19} \frac{J_1}{kT_L}\right)^{1/2} J_1 \Delta p^3 \quad . \quad (IV.20)$$

These results show that, at the Lifshitz point, the two lines of tricritical points have a common tangent with the lines $T_\lambda(p)$, $T_o(p)$ and $T_1(p)$, determined in the last chapter. This feature of the tricritical lines can be seen in Fig. 4.

In general, the expression for the tricritical temperature (IV.17) is not valid for all p , since it may become negative for large p . It is necessary, therefore, to investigate the stability of the tricritical points. This will be done, in the next section, in the context of Landau's theory of phase transitions.

V. THE LANDAU THEORY IN NON-ZERO FIELDS

The mean-field expression for the Gibbs free-energy is analytic in δm_z , defined by Eq. (IV.2), and may be

expanded in the form

$$N^{-3}G_{MF}(T,H,N;\{\delta m_z\}) = N^{-3}G_o + \sum_z \left\{ -\frac{1}{2}\left[4J_o\ \delta m_z^2 + \right.\right.$$

$$+ J_1\ \delta m_z(\delta m_{z-1} + \delta m_{z+1}) + J_2\ \delta m_z(\delta m_{z-2} + \delta m_{z+2})\Big] +$$

$$+ \frac{1}{2}A\ \delta m_z^2 + \frac{1}{3}B\ \delta m_z^3 + \frac{1}{4}C\ \delta m_z^4 + \frac{1}{5}D\ \delta m_z^5 +$$

$$\left. + \frac{1}{6}E\ \delta m_z^6 + \ldots\right\} \quad , \tag{V.I}$$

where G_o , A , B ,...., E are functions of T and H given by

$$G_o = N^3\left\{-kT\ \ell n\ 2 + \frac{1}{2}kT\left[(1+m_o)\ \ell n\ (1+m_o) + \right.\right.$$

$$\left.\left. + (1-m_o)\ \ell n\ (1-m_o)\right] - \frac{1}{2}J(0)\ m_o^2\right\} \tag{V.2}$$

$$A = \frac{kT}{1 - m_o^2} \tag{V.3}$$

$$B = kT\ \frac{m_o}{(1 - m_o^2)^2} \tag{V.4}$$

$$C = kT\ \frac{1 + 3m_o^2}{3(1 - m_o^2)^3} \tag{V.5}$$

$$D = kT\ \frac{m_o(1 + m_o^2)}{(1 - m_o^2)^4} \tag{V.6}$$

$$E = kT \frac{1 + 10m_o^2 + 5m_o^4}{5(1 - m_o^2)^5} \quad . \tag{V.7}$$

By representing δm_z in terms of its Fourier components as in expression (IV.4), we may write the expansion of the free-energy in the form

$$N^{-3} G_{MF}(T,H,N;\{m_q\}) = N^{-3} G_o +$$

$$+ \frac{1}{2} \sum_{q_1 q_2} \left[A - J(q_1)\right] m_{q_1} m_{q_2} \Delta(q_1 + q_2) +$$

$$+ \frac{1}{3} B \sum_{q_1 q_2 q_3} m_{q_1} m_{q_2} m_{q_3} \Delta(q_1 + q_2 + q_3) +$$

$$+ \frac{1}{4} C \sum_{q_1 q_2 q_3 q_4} m_{q_1} m_{q_2} m_{q_3} m_{q_4} \Delta(q_1 + q_2 + q_3 + q_4) + \ldots \tag{V.8}$$

where the Δ function, defined by

$$\Delta(q) = \sum_{n=-\infty}^{\infty} \delta(q + 2\pi n) \tag{V.9}$$

expresses the wave vector conservation (modulo 2π).

To obtain the expansion of G up to the sixth order term in the order parameter, it is enough to consider up to the third harmonic component in δm_z. As in the last chapter, let us call

$$m_o = M_o \quad ; \quad 2m_{nq_c} = M_n e^{i\phi_n} \quad (n \geq 1) \tag{V.10}$$

where, for convenience, M_o , M_1 , M_2 , ... are supposed real. Disregarding the possibility of umklapp terms we have

$$\begin{aligned} N^{-3}G = N^{-3}G_o &+ \tfrac{1}{2} A_o M_o^2 + \tfrac{1}{4} A_1 M_1^2 + \\ &+ \tfrac{1}{4} A_2 M_2^2 + \tfrac{1}{4} A_3 M_3^2 + B \left\{ \tfrac{1}{3} M_o^3 + \right. \\ &+ \tfrac{1}{4} M_1^2 M_2 \cos(\phi_2 - 2\phi_1) + \tfrac{1}{2} M_o M_1^2 + \\ &+ \left. \tfrac{1}{2} M_o M_2^2 + \tfrac{1}{2} M_1 M_2 M_3 \cos(\phi_3 - \phi_2 - \phi_1) \right\} + \\ &+ C \left\{ \tfrac{3}{32} M_1^4 + \tfrac{3}{4} M_o^2 M_1^2 + \tfrac{3}{8} M_1^2 M_2^2 + \right. \\ &+ \left. \tfrac{1}{8} M_1^3 M_3 \cos(\phi_3 - 3\phi_1) + \tfrac{3}{4} M_o M_1^2 M_2 \cos(\phi_2 - 2\phi_1) \right\} + \\ &+ D \left\{ \tfrac{1}{4} M_1^4 M_2 \cos(\phi_2 - 2\phi_1) + \tfrac{3}{8} M_o M_1^4 \right\} + \tfrac{5}{96} E M_1^6 \ , \end{aligned} \tag{V.11}$$

where

$$A_n = A - J(nq_c) \quad . \tag{V.12}$$

The minimization of G with respect to M_o , M_2 and M_3 gives

$$M_o \approx a_o M_1^2 + b_o M_1^4 \quad , \tag{V.13}$$

$$M_2 \approx a_2 M_1^2 + b_2 M_1^4 \quad , \tag{V.14}$$

$$M_3 \approx a_3 M_1^3 \quad , \tag{V.15}$$

where

$$a_o = -\frac{B}{2A_o} \quad , \tag{V.16}$$

$$b_o = \frac{1}{8A_o}\left\{\frac{6BC}{A_o} + \frac{3BC}{A_2} - \frac{2B^3}{A_o^2} - \frac{B^3}{A_2^2} - 3D\right\} \quad , \tag{V.17}$$

$$a_2 = -\frac{B}{2A_2} \quad , \tag{V.18}$$

$$b_2 = \frac{1}{8A_2}\left\{\frac{6BC}{A_o} + \frac{6BC}{A_2} + \frac{2BC}{A_3} - \frac{4B^3}{A_oA_2} - \frac{4B^3}{A_2A_3} - 4D\right\} \quad , \tag{V.19}$$

$$a_3 = \frac{1}{4A_3}\left(\frac{2B^2}{A_2} - C\right) \quad . \tag{V.20}$$

The phase ϕ_1 is arbitrary, but the other phases are fixed according to $\phi_n = n\phi_1$. Inserting expressions (V.13) to (V.15) into Eq. (V.11) we have the expansion

$$N^{-3}G(T,H,N;M_1) = N^{-3}G_o(T,H,N) + C_2(T,H)M_1^2 +$$

$$+ C_4(T,H)M_1^4 + C_6(T,H)M_1^6 + \ldots \qquad (V.21)$$

where

$$C_2 = \frac{1}{4} A_1 \quad , \qquad (V.22)$$

$$C_4 = -\frac{B^2}{16}\left(\frac{2}{A_o} + \frac{1}{A_2}\right) + \frac{3}{32} C \quad , \qquad (V.23)$$

$$C_6 = -\frac{B^4}{16}\left(\frac{2}{3A_o^3} + \frac{1}{A_o A_2^2} + \frac{1}{A_2^2 A_3}\right) + \frac{B^2 C}{32}\left(\frac{6}{A_o^2} + \frac{6}{A_o A_2} + \frac{3}{A_2^2} + \frac{2}{A_2 A_3}\right) -$$

$$- \frac{BD}{16}\left(\frac{3}{A_o} + \frac{2}{A_2}\right) - \frac{C^2}{64A_3} + \frac{5}{96} E \quad . \qquad (V.24)$$

The critical surface and the lines of tricritical points are determined by the conditions $C_2 = 0$ with $C_4 > 0$, and $C_2 = C_4 = 0$ with $C_6 > 0$, respectively. Needless to say, in this way we obtain the expressions which had already been calculated in the last section. The condition $C_6 > 0$ ceases to be satisfied for a sufficiently large value of the parameter p. When $C_2 = C_4 = C_6 = 0$ and $C_8 > 0$ a new kind of multicritical point emerges, which corresponds to the limit of stability of the line of tricritical points[13]. In the particular case $J_o = J_1$ this multicritical points was found to occur at $p = 2.946\ldots$. For still larger values of the parameter p the system exhibits two distinct endpoints, namely, the critical endpoint and the bicritical endpoint, in analogy with metamagnetic systems[13]. This behavior was

observed in the numerical calculations for the case $p = 4$, as will be discussed in the next section.

Finally, we observe that when umklapp terms are present they should be taken into account. However, for the particular case $J_1 > 0$ in which we are interested, the umklapp terms have no influence on the location of the tricritical points.

VI. NUMERICAL RESULTS IN THE MODULATED PHASE

In the preceding sections we have examined the properties of the model near the critical surface. It was shown that the modulated phase in this region is a distorted sinusoidal wave with the periodicity determined by the parameter $p = -J_2/J_1$. As the temperature is decreased, however, transitions may occur to other modulated phases. Indeed, at zero field, it is known that this model presents a large number of distinct modulated phases[8,9]. In this sections we show, through numerical calculations, the main features of the effects of an applied field on the modulated phases.

Within the mean-field approximation, the problem consists in the solution of the infinite number of coupled nonlinear equations (II.10). Since it is not possible to obtain a general analytic solution, we have to resort to numerical calculations[9,11]. Let us suppose that the solution is periodic with a periodicity of L lattice spacings. With this assumption, the infinite system of equations (II.10) reduces to a system of L coupled equations, which can be solved self-consistently.

As initial configurations we may use sinusoidal structures with different periodicities. In this way periodic solutions with periodicity L are obtained. In the calculations we restricted ourselves to the particular case $J_o = J_1 > 0$, $J_2 < 0$, and $H > 0$. Moreover, we considered only periodicities of up to 20 lattice spacings, that is, we examined solutions with wave vectors of the form $q = 2\pi K/L$, where $0 \leq K < L \leq 20$. Among the various solutions found for a given point in the T-p-H space, only that one which minimizes the free-energy is physically relevant. Needless to say, the procedure just described does not take into account all the possible commensurate phases, not to mention the incommensurate ones. Therefore, our results are limited to the main commensurate phases, and it is to be understood that in between them there may exist other commensurate or incommensurate phases.

Some of the average spin configurations found in the presence of a field are shown in Fig. 5. Fig. 5a shows the average spin configuration of the modulated phase with wave vector $q = 2\pi/5$. To better characterize this phase we will adopt the notation $\langle 32 \rangle$, which means that three planes with spins predominantly parallel to the field are followed by two planes of spins predominantly antiparallel to the field[8] . According to this notation, Figs. 5b and 5c correspond to the average spin configurations of the modulated phases $\langle 3332 \rangle \equiv \langle 3^3 2 \rangle$ and $\langle 32^3 32 \rangle$. The continuous curves superimposed on these figures show the sum of the zeroth and the first harmonic components of the magnetization. It is clear from these figures that the magnetic field has the effect

of inhibiting the occurence of antiparallel spins, thereby producing a net total magnetization parallel to the field. It can also be seen that there are, in general, significant contributions of the higher harmonic components to the magnetization.

Phase diagrams in the T-H plane, for three representative values of p, are shown in Figs. 6, 7 and 8. In the case $p = 0.4$, shown in Fig. 6, the ground state is ferromagnetic, and the modulated phase is limited to a hump-shaped region which is stable only for small fields. This observed behavior for $p = 0.4$ is characteristic of all T-H phase diagrams for which $0.25 < p < 0.5$. In the case $p = 0.6$, shown in Fig. 7, the ground state in the modulated phase is the (2,2) antiphase state, denoted by <2> in the notation introduced previously (see Appendix B). Notice that the modulated phase is dominated by the simple commensurate phases with wave vectors $q/2\pi = 1/4, 1/5, 3/16$ and $2/11$. It is interesting to observe that the modulated phases <3> and $<23^5>$ are limited to a small region of very weak fields. This fact is probably related to the non-monotonic behavior of the wave vector for $p = 0.6$ and to the bulging of the phase <3> observed in the T-p phase diagram[9]. Finally, the T-H phase diagram for a large value of the parameter p, namely $p = 4$, is shown in Fig. 8. We can observe that the modulated phase is overwhelmingly dominated by the (2,2) antiphase. Indeed, in our numerical calculations we did not find any other phases except the (2,2) antiphase. This is due to the limitations of the numerical calculations discussed previously, since

we know that close to the λ-surface the modulated structure has the wave vector determined by Eq. (IV.6). Furthermore, a detailed numerical study near the λ-surface was hindered by the fact that the convergence of the numerical process may become very slow. The fact that the phase diagram for $p = 4$ is almost fully occupied by the (2,2) antiphase is not surprising, since for large p the model can be imagined as consisting of two weakly coupled interpenetrating metamagnetic systems. Notice that in this case the first-order transition line does not meet tangentially with the λ-line, but it penetrates into the modulated region, becoming a line of coexistence of two (2,2) antiphases. The endpoints of the λ-line and of the first-order transition line are the critical endpoint and the bicritical endpoint, respectively, in analogy with metamagnetic systems[13].

The behavior of some thermodynamic functions when the system passes through different modulated phases was also examined. Fig. 9 shows the graph of the entropy as a function of temperature for zero applied field and $p = 0.6$. It should be remarked that in between the main commensurate phases the system undergoes a number of first-order phase transitions to other less stable commensurate phases. It has been suggested that the corresponding curve of the wave vector as a function of temperature could be an example of the devil's staircase[9,11]. This means that the wave vector as a function of temperature would be, for a certain temperature interval, continuous, monotonic and with zero derivative almost every-where[16]. Whether this model can diplay a true devil's

staircase behavior or not has been a subject of various studies[8,17,18], and it is not our intention to deal with this complex and subtle problem. In any event, there is no possibility of identifying the true devil's staircase numerically, and our use of the term devil's staircase does not imply that we are claiming to have found a true devil's staircase as defined by the mathematicians[16]. In Fig. 10 we show a graph of the magnetization as a function of the applied field for $p = 0.6$ and $(k_B T/J_1) = 2.75$. By refining the numerical calculations between the commensurate phases <2> and <32>, a number of other modulated phases were found. Therefore, the devil's staircase picture is likely to hold as a function of either temperature or applied field.

VII. SUMMARY AND CONCLUSIONS

We have studied a layered Ising model with competing interactions between nearest and next-nearest layers in the presence of an applied magnetic field. All the calculations were performed within the mean-field approximation in which distinct effective fields are assigned to each plane. The λ-surface, and the ordered region just below it, were studied analytically by means of the standard mean-field techniques and the Landau theory of second-order phase transitions. The modulated structure near the λ-surface is a distorted sinusoidal wave with a period determined by the ratio p of the competing interactions. Commensurate structures, in which the period is an integral multiple of the

lattice spacing, are pinned to the lattice by the umklapp terms, whereas incommensurate structures can undergo a free translation relative to the lattice without changing the free--energy. Both odd and even higher harmonic components are present in non-zero fields, as opposed to the case of zero fields where only odd higher harmonic components are present. The n-th order harmonic component depends asymptotically on the n-th power of the main harmonic component. The λ-surface is bounded by two lines of tricritical points which join smoothly at the Lifshitz point and end at multicritical points for a particular value of the parameter p , beyond which lines of critical and bicritical endpoints are expected to appear. The modulated phases at low temperatures were studied by means of a direct numerical analysis of the mean-field equations. Some modulated phases which are present at zero field were found to be stable only for very weak fields. The modulated phases in the T-H plane for $0.25 < p < 0.5$ are limited to a hump-shaped region, while for larger values of the parameter p they become increasingly dominated by the (2,2) antiphase. The devil's staircase behavior is likely to occur either as a function of the temperature or the magnetic field. At least in principle, some steps of the devil's staircase should be amenable to an experimental observation, in the magnetization measurements, as a series of first-order transitions taking place in a very narrow field interval. Finally, we would like to point out that our results have the well known defficiencies of the mean-field theories. Moreover, the numerical calculations

are further restricted by the fact that only the main commensurate structures were taken into account. Notwithstanding these limitations, we believe that the main qualitative conclusions, in particular those concerning the phase diagrams, are correct.

ACKNOWLEDGMENT

It is a pleasure to thank Dr. Walter Selke for many useful comments and for keeping us informed about his and related works on the subject area of this paper. Also, we wish to acknowledge Prof. Marco A. de Moura for stimulating conversations in the beginning of these investigations. We are indebted to the Brazilian agencies FAPESP, CNPq, and FINEP for the financial support of the research reported here. One of us (MDC) appreciated the hospitality of the Instituto de Física of the Universidade de São Paulo.

APPENDIX A - THE LANDAU THEORY IN ZERO FIELD

A.1 - Results near the Lifshitz point.

Magnetic systems with uniaxial spontaneous magnetization were studied by Michelson[19], in the vicinity of the Lifshitz point, on the basis of Landau's theory of second-order phase transitions. The Ising model considered in this paper is probably the simplest possible realization of a uniaxial system exhibiting a Lifshitz point. To facilitate the comparison, we will obtain the phenomenological coefficients of Michelson's work as a function of the microscopic parameters of the model.

Substitution of the Fourier decomposition of the layer magnetization (III.2) into the expansion of the free-energy (III.17) gives

$$N^{-3}G = - kT\ \ell n\ 2 + \sum_{q_1,q_2} \frac{1}{2}\left[kT - J(q)\right] m_{q_1}\, m_{q_2}\, \Delta(q_1+q_2) +$$

$$+ \sum_{n=2}^{\infty} \frac{1}{2n(2n-1)}\, kT \sum_{q_1,\ldots,q_{2n}} m_{q_1} \ldots m_{q_{2n}}\, \Delta(q_1+\ldots+q_{2n}) \,. \qquad (A.1)$$

Near the Lifshitz point the umklapp terms can be neglected. Hence we have

$$N^{-3}G = -kT\,\ell n\,2 + \frac{1}{2}\sum_{q} A_q\,|mq|^2 + \frac{1}{4}B' \sum_{q_1+\ldots+q_4=0} m_{q_1}\ldots m_{q_4} +$$

$$+ \frac{1}{6}C' \sum_{q_1+\ldots+q_6=0} m_{q_1}\ldots m_{q_6} + \ldots \quad , \qquad (A.2)$$

where, in Michelson's notation,

$$A_q = kT - J(q) = A_o + \alpha q^2 + \frac{1}{2}\beta q^4 + \ldots \quad ,$$

$$A_o = kT - (4J_o + 2J_1 + 2J_2) \quad ,$$

$$\alpha = J_1\,(1 - 4p) \quad ,$$

$$\beta = -\frac{1}{6}J_1(1 - 16p) \quad ,$$

$$B' = \frac{1}{3}kT \qquad ; \qquad C' = \frac{1}{5}kT \qquad (A.3)$$

The properties of the model near the Lifshitz point are described by Michelson's results with the coefficients of the Landau expansion given by Eqs. (A.3).

A.2 - Effect of the umklapp terms.

Away from the Lifshitz point, umklapp terms may become relevant for commensurate wave vectors. Indeed, as pointed out in section III.B, umklapp terms are responsible for the pinning of commensurate phases with respect to the

lattice. To illustrate this point, let us consider, for instance, the commensurate phase with wave vector $q_c = \pi/3$. This phase is realized, below T_c, for $p = 1/2$. For this value of q_c the magnetization may be written as the finite Fourier series

$$m_z = m_{q_c} e^{iq_c z} + m_{-q_c} e^{-iq_c z} + m_{3q_c} e^{i3q_c z} , \quad (A.4)$$

where only the odd harmonic components are present. By substituting Eq. (A.4) into Eq. (A.1), and keeping only the terms up to sixth order we obtain

$$N^{-3}G = - kT \ell n\, 2 + \frac{1}{4} A_1 M_1^2 + \frac{1}{2} A_3 M_3^2 +$$

$$+ \frac{1}{12} kT \left\{ \frac{3}{8} M_1^4 + M_3 M_1^3 \cos 3\phi_1 \right\} +$$

$$+ \frac{1}{960} kT \left\{ 10 M_1^6 + M_1^6 \cos 6\phi_1 \right\} + \ldots , \quad (A.5)$$

where A_n is defined in Eq. (V.12), and as usual we have put

$$2m_{q_c} = M_1 e^{i\phi_1} \quad ; \quad m_{3q_c} = M_3 . \quad (A.6)$$

Now, the minimization of G with respect to M_3 gives in leading order

$$M_3 \approx - \frac{kT}{12A_3} M_1^3 \cos 3\phi_1 , \quad (A.7)$$

and the free-energy expansion takes the form

$$N^{-3}G = - kT \ln 2 + \frac{1}{4} A_1 M_1^2 + \frac{1}{32} kT M_1^4 +$$

$$+ \frac{1}{192} kT \left\{2 - \frac{1}{3}\frac{kT}{A_3} + \left(\frac{1}{5} - \frac{1}{3}\frac{kT}{A_3}\right) \cos 6\phi_1\right\} M_1^6 + \ldots \quad (A.8)$$

The phase ϕ_1 has to be chosen so as to give the lowest possible value for the free-energy. The above expansion shows that, near T_c , ϕ_1 is determined by the sixth order term according to the sign of

$$\frac{1}{5} - \frac{1}{3}\frac{kT}{A_3} \approx \frac{4}{45} - \frac{8}{27}\frac{J_o}{J_1} \quad . \qquad (A.9)$$

Thus, for $J_o > 0.3J_1$, $\phi_1 = 0 \pmod{\pi/3}$ whereas for $J_o < 0.3J_1$, $\phi_1 = \pi/6 \pmod{\pi/3}$.

Generally speaking, commensurate phases of the form $q = 2\pi K/L$ are pinned with respect to the lattice by the L-th order umklapp terms. For incommensurate wave vectors, the phase of the main harmonic component is arbitrary, and the modulated phase can undergo a free translation relative to the lattice without changing the free-energy

APPENDIX B - GROUND STATE

The ground state of the model, in the mean-field approximation, can be determined by minimizing the zero temperature free-energy

$$N^{-2} G_{MF}(T=0,H;\{m_z\}) = -\frac{1}{2} \sum_z \left\{ 4J_o\, m_z^2 + J_1\, m_z (m_{z-1} + m_{z+2}) + \right.$$

$$\left. + J_2\, m_z (m_{z-2} + m_{z+2}) \right\} - H \sum_z m_z \quad , \qquad (B.1)$$

where the layer magnetization m_z is limited to the values ± 1 . Since the spins in each layer interact ferromagnetically, expression (B.1) also gives the exact ground state energy of the model. The problem of finding the ground state reduces, therefore, to that of finding the ground state of the one dimensional Ising model described by the Hamiltonian

$$\mathcal{H} = - \sum_{z=1}^{N} (J_1\, \sigma_z\, \sigma_{z+1} + J_2\, \sigma_2\, \sigma_{z+2} + H\, \sigma_z) \quad , \qquad (B.2)$$

where σ_z corresponds to m_z . This problem can be solved by the transfer matrix method or by a direct counting of possible spin arrangements[20]. The latter method gives for the ground state energy per spin the result

$$E = \min \left\{ \epsilon_+ \, , \, \epsilon_- \, , \, \epsilon_{+-} \, , \, \epsilon_{+--} \, , \, \epsilon_{+-+} \, , \, \epsilon_{+--+} \right\} \qquad (B.3)$$

where

$$\epsilon_\pm = - J_1 - J_2 \mp H$$

$$\epsilon_{+-} = J_1 - J_2$$

$$\epsilon_{+--} = (J_1 + J_2 + H)/3$$

$$\epsilon_{+-+} = (J_1 + J_2 - H)/3$$

$$\epsilon_{+--+} = J_2 \qquad \text{(B.4)}$$

The ground state spin configuration is a sequence of groups of spins as indicated in the index of the minimum ϵ. For example, if ϵ_{+--+} has the lowest energy, then the ground state is the sequence $+--++--+...$, that is, the (2,2) antiphase state. The possible ground-states in zero fields are shown in Fig. 2. The ground-state is metamagnetic for $J_1 < 0$ and $J_2 > 0.5\, J_1$, ferromagnetic for $J_1 > 0$ and $J_2 > -0.5\, J_1$, and the (2,2) antiphase state for $J_2 < 0$ and $|J_1| < 2|J_2|$. For arbitrary H and $J_1 > 0$, the ferromagnetic and the (2,2) antiphase states are the only possible ground states, as shown in Fig. 11. However, we remark that for $J_1 < 0$ other ground states are possible.

Of particular interest are the transition lines separating the (2,2) antiphase from the ferromagnetic phases in Fig. 11. On the transition line $H = J_1(-1 + 2p) > 0$ we have $\epsilon_+ = \epsilon_{+--+}$, and infinitely many ground states can be constructed from the arbitrary arrangement of groups of spins + and $+--+$. The ground state degeneracy D_n , in the thermodynamic limit, is given by

$$\lim_{N\to\infty} \frac{1}{N} \ln D_N = \ln x = 0.32228... \quad , \qquad (B.5)$$

where x is the solution of the quartic equation $x^3(x-1) = 1$. Due to symmetry, on the transition line $H = J_1(1-2p) < 0$ we have the same ground state degeneracy with the possible ground states constructed from the arrangements of groups of spins - and -++- . Finally, on the point of intersection of the two transition lines, that is, at the multiphase point $(p,H) = (1/2,0)$, the ground state is even more degenerate. Possible ground states have a sequence of at least two "up" spins followed by at least two "down" spins. The ground state degeneracy D_N is given by the recursion relation of Fibonacci's sequence, and one has in the thermodynamic limit[15],

$$\lim_{N\to\infty} \frac{1}{N} \ln D_N = \ln \left(\frac{1+\sqrt{5}}{2}\right) = 0.48121... \qquad (B.6)$$

We can observe that there is a residual entropy on these transition lines in the case of one dimensional systems, but not for higher dimensional systems.

APPENDIX C - THE SPHERICAL MODEL

The spherical version of the Ising model considered in this paper exhibits a Lifshitz point, and its multicritical behavior was analysed in detail by Hornneich et al[21]. In view of the results obtained for the Ising model,

it is instructive to consider the spherical version in the presence of an applied field.

The mean-spherical model partition function is[22]

$$\underline{\underline{Z}}\,(\beta,H,\mu) = \prod_{xyz}\left(\int_{-\infty}^{+\infty} d\sigma_{xyz}\right)\exp\left[-\beta\mathcal{H} - \beta\mu\sum_{xyz}\sigma_{xyz}^2\right] \quad , \qquad (C.1)$$

where $\mathcal{H}$ is the Hamiltonian (II.1) but with the spin variables ranging from $-\infty$ to $+\infty$. The chemical potential μ should be determined from the so-called spherical condition

$$\left\langle \sum_{xyz}\sigma_{xyz}^2 \right\rangle = -\frac{1}{\beta}\frac{\partial}{\partial\mu}\ell n\,\underline{\underline{Z}} = N^3 \qquad (C.2)$$

As it is well known, at and below the transition temperature the chemical potential sticks to its critical value, which is given by

$$\mu_c = \max_{\vec{q}}\left\{\frac{1}{2}J(\vec{q})\right\} = \frac{1}{2}J(\vec{q}_c) \quad , \qquad (C.3)$$

where

$$J(\vec{q}) = 2J_o(\cos q_x + \cos q_y) + 2J_1\cos q_z + 2J_2\cos 2q_z \; . \qquad (C.4)$$

Here we will limit ourselves to the case $J_o, J_1 > 0$, $J_2 < 0$,

and, as usual, introduce the field parameter $p = -J_2/J_1$. Then, as in Sec. III, we have a ferromagnetic ordering $\vec{q}_c \equiv 0$ for $p < 1/4$, and a modulated ordering $\vec{q}_c = (0,0,q_c)$, with q_c given by Eq. (III.6), for $p > 1/4$. The Lifshitz point occurs at $p = 1/4$. The paramagnetic-ferromagnetic λ-line in zero field, $T_o(p)$, is given by

$$\frac{kT_o(p)}{(2\pi)^3} \int \frac{d^3\vec{q}}{J(0) - J(\vec{q})} = 1 \quad . \tag{C.5}$$

No phase transition occurs for $p < 1/4$ in non zero-fields. For $p > 1/4$, however, there exists a phase transition even in non-zero fields. The paramagnetic-modulated λ-line becomes the λ-surface $T_\lambda(p,H)$ determined by

$$\frac{H^2}{\left[J(\vec{q}_c) - J(0)\right]^2} + \frac{kT_\lambda(p,H)}{(2\pi)^3} \int \frac{d^3\vec{q}}{J(\vec{q}_c) - J(\vec{q})} = 1 \ . \tag{C.6}$$

The net magnetization per spin in the paramagnetic phase is

$$M = \frac{H}{2\left[\mu - \frac{1}{2} J(0)\right]} \quad , \tag{C.7}$$

whereas in the ordered phase

$$M = \frac{H}{2\left[\mu_c - \frac{1}{2} J(0)\right]} \tag{C.8}$$

At the transition surface μ is equal to p_c. Therefore, the magnetization varies continuously through the transition surface, which confirms its second-order nature. The non-existence of tricritical behavior is not surprising, since this is already the case of a metamagnetic spherical system[23]. The form of the λ-surface is given by Eq. (C.6), which may also be written as

$$\frac{T_\lambda(p,H)}{T_\lambda(p,0)} = 1 - \frac{H^2}{J_1^2} \frac{16p^2}{(1-4p)^4} \qquad \text{(C.9)}$$

Eq. (C.9) emphasizes, for fixed p, the usual parabolic shape of the transition line found in spherical models.

REFERENCES

1. R.M. Hornreich, M. Luban, and S. Shtrikman, Phys. Rev. Lett. 35, 1678 (1975).

2. See, e.g., N.L. McMillan, Phys. Rev.B 14, 1496 (1976); P. Bak and V.J. Emery, Phys. Rev. Lett. 36, 978 (1976); A.D. Bruce, R.A. Cowley and A.F. Murray, J. Phys.C 11, 3591 (1978).

3. R.J. Elliot, Phys. Rev. 124, 346 (1961). For similar models see, e.g., T.A. Kaplan, Phys. Rev. 124, 329 (1961); H. Miwa and K. Yosida, Progr. Theoret. Phys. (Kyoto) 26, 693 (1961); J. Jensen, J. Phys. F 6, 1145 (1976).

4. M. Droz and M.D. Coutinho-Filho, AIP Conf. Proc. Nº 29 (AIP, New York, 1976), p. 465. See also R.M. Hornreich, J. Magn. Mag. Matls. 15 - 18, 387 (1980) and references quoted therein.

5. S. Redner and H.E. Stanley, Phys. Rev. B 16, 4901 (1977); J. Phys. C 10, 4765 (1977).

6. W. Selke, Z. Phys. B 29, 133 (1978); J. Phys. C 13, L261 (1980).

7. W. Selke and M.E. Fisher, Phys. Rev. B 20, 257 (1979); J. Magn. Mag. Matls. 15 - 18, 403 (1980).

8. M.E. Fisher and W. Selke, Phys. Rev. Lett. 44, 1502 (1980); Proc. Roy. Soc. to be published. The name ANNNI model has been introduced in these papers to characterize the axial next-nearest neighbor Ising model which we are considering.

9. P. Bak and J. von Boehm, Phys. Rev. B 21, 5297 (1980).

10. P. Fisher, B. Lebech, G. Meier, B.D. Rainford and O. Vogt, J. Phys. C 11, 345 (1978).

11. J. von Boehm and P. Bak, Phys. Rev. Lett. 42, 122 (1979).

12. C.C. Becerra, Y. Shapira, N.F. Oliveira Jr. and T.S. Chang, Phys. Rev. Lett. 44, 1692 (1980).

13. J.M. Kincaid and E.G.D. Cohen, Phys. Rep. 22, 57 (1975).

14. See, e.g., H. Falk, Am. J. Phys. 38, 858 (1970).

15. W. Selke and M.E. Fisher, Z. Phys. B 40, 71 (1980).

16. B.B. Mandelbrot, Fractals: Form, Change and Dimension (Freeman, San Francisco, 1977).

17. J. Villain and M.B. Gordon, J. Phys. C 13, 3117 (1980).

18. E.B. Rasmussen and S.J. Knak Jensen, to be published.

19. A. Michelson, Phys. Rev. B 16, 577 (1977). A generalization of these results in the presence of an applied field, but neglecting higher harmonic components of the magnetization, has recently been presented by M.D. Coutinho-Filho and Marco A. de Moura, J. Magn. Mag. Mat. 15-18, 433 (1980).

20. T. Morita and T. Horiguchi, Phys. Lett. 38A, 223 (1972).

21. R.M. Hornreich, M. Luban and S. Shtrikman, Physica 86A, 465 (1977).

22. See, e.g., G.S. Joyce, in Phase Transitions and Critical Phenomena, edited by C. Domb and M.S. Green (Academic, New York, 1972), Vol. 2, p. 375.

23. H.J. Knops, Phys. Rev. B 8, 4209 (1973).

FIGURE CAPTIONS

FIG.1 Ising model with ferromagnetic coupling J_o within each layer and competing couplings J_1 and J_2 between nearest and next-nearest layers, respectively.

FIG.2 Projection of the regions of ordered phases found at $T = T_c$ and $T = 0$, in zero field, onto the J_2 vs. J_1 plane. The solid lines separate the three ordered phases found just below T_c, whereas the dashed lines separate the ferromagnetic, metamagnetic and (2,2) antiphase states found at $T = 0$. $J_1 \pm 4J_2 = 0$ are projections of the lines of Lifshitz points, while $J_1 \pm 2J_2 = 0$ are lines of multiphase points.

FIG.3 Phase diagram of the model near the Lifshitz point (T_L, p_L), as determined from the asymptotic expressions. The dot-dashed line is the projection of the tricritical lines on the T-p plane. The insert shows a larger region around the Lifshitz point (LP), for the case $J_o = J_1$, which separates the paramagnetic (PM), ferromagnetic (FM) and modulated (M) phases.

FIG.4 Phase diagram of the model for the case $J_o = J_1$, in the presence of an applied magnetic field. The dash--dotted lines of tricritical points separate the second-order transition surface from the first-order transition surface (indicated by dotted lines). The lines of tricritical points end at $p = 2.946...$. For larger values of p, lines of critical and bicritical endpoints, which are not shown, are expected to appear. Inside the modulated region there exist many distinct modulated phases, but they are not shown in this picture.

FIG.5 Various plots of the magnetization per spin in a layer m_z, as a function of the layer coordinate z, which were found numerically for the case $J_o = J_1$ in non-zero fields. The continuous curve represents the sum of the zeroth and first harmonic components.

FIG.6 Temperature vs. magnetic field phase diagram as determined numerically for the case $J_o = J_1$ and $p = 0.4$. The heavy line is a second-order transition line ending at the tricritical point (TCP).

FIG.7 Temperature vs. magnetic field phase diagram as determined numerically for the case $J_o = J_1$ and $p = 0.6$. The heavy line is a second-order transition line ending at the tricritical point (TCP). The insert shows the details around the phase <3>.

FIG.8 Temperature vs. magnetic field phase diagram as determined numerically for the case $J_o = J_1$ and $p = 4$. The heavy line is a second-order transition line ending at the critical endpoint (CE). The insert shows the details around the bicritical endpoint (BCE), which was determined numerically.

FIG.9 Graph of the entropy as a function of temperature in zero field for the case $J_o = J_1$ and $p = 0.6$. The insert shows the details of the transition between the phases <2> and <3>.

FIG.10 Graph of the net magnetization per spin vs. applied magnetic field for the case $J_o = J_1$, $p = 0.6$ and $kT/J_1 = 2.75$. The insert shows the details of the transition between the phases <2> and <3>.

FIG.11 Ground-state of the model in non-zero fields for the case $J_1 > 0$. The (2,2) antiphase state is separated from the ferromagnetic phases by the lines $H = \pm J_1 (2p-1)$, which meet at the multiphase point (MP).

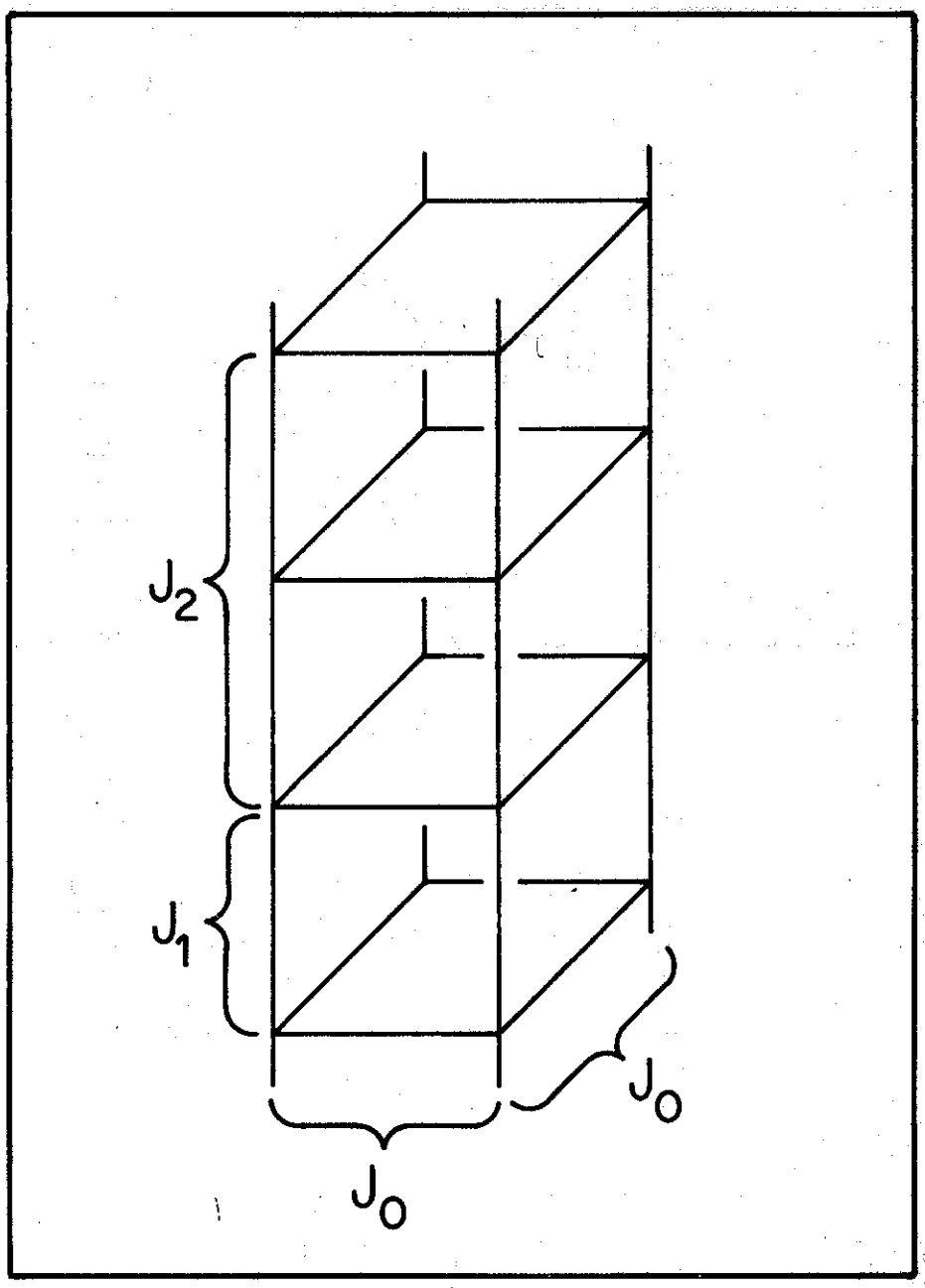

FIG. 1

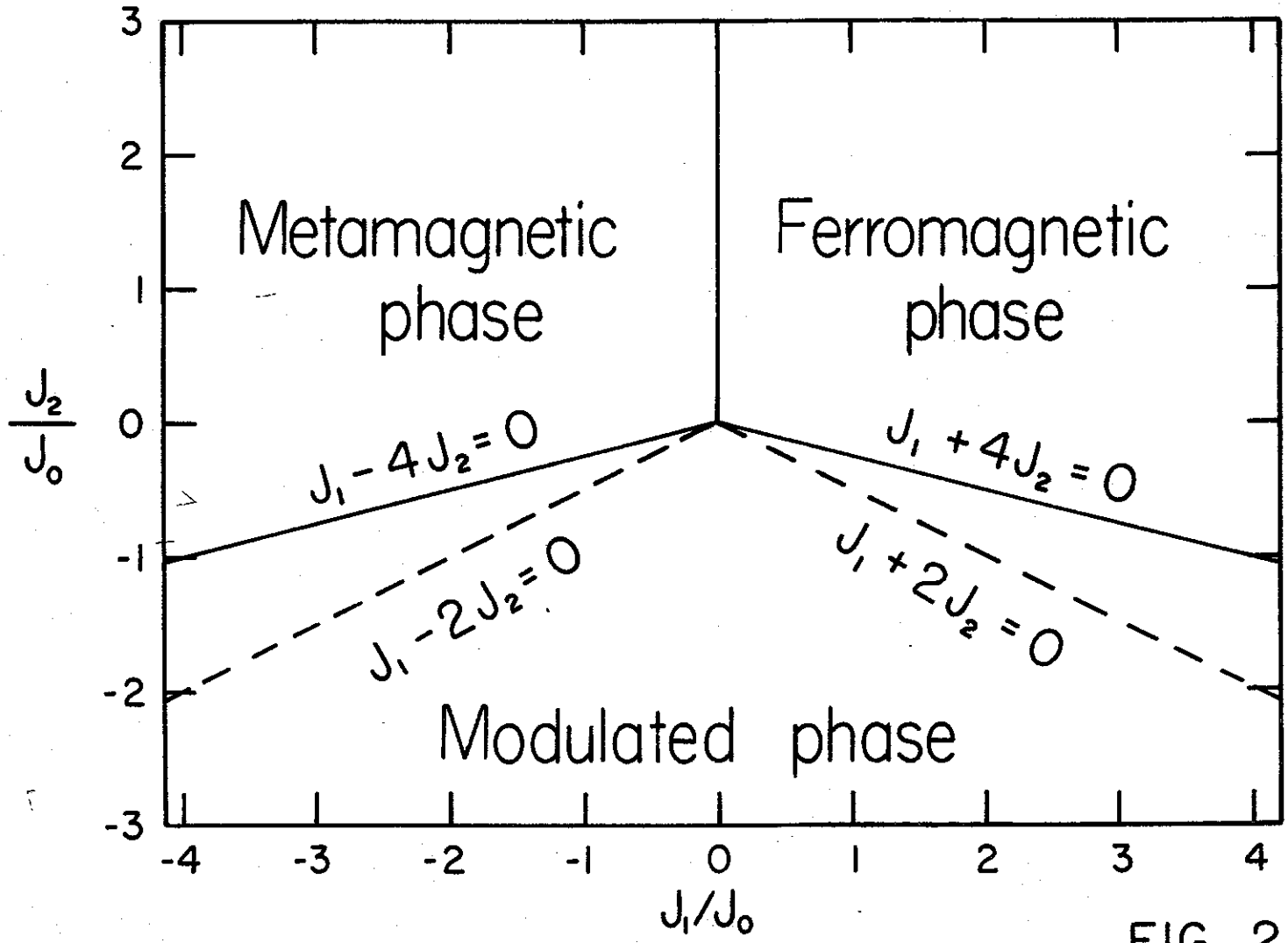
Metamagnetic phase
Ferromagnetic phase
Modulated phase
$J_1 - 4J_2 = 0$
$J_1 + 4J_2 = 0$
$J_1 - 2J_2 = 0$
$J_1 + 2J_2 = 0$
$\frac{J_2}{J_0}$
J_1/J_0
3
2
1
0
-1
-2
-3
-4
-3
-2
-1
0
1
2
3
4

FIG. 2

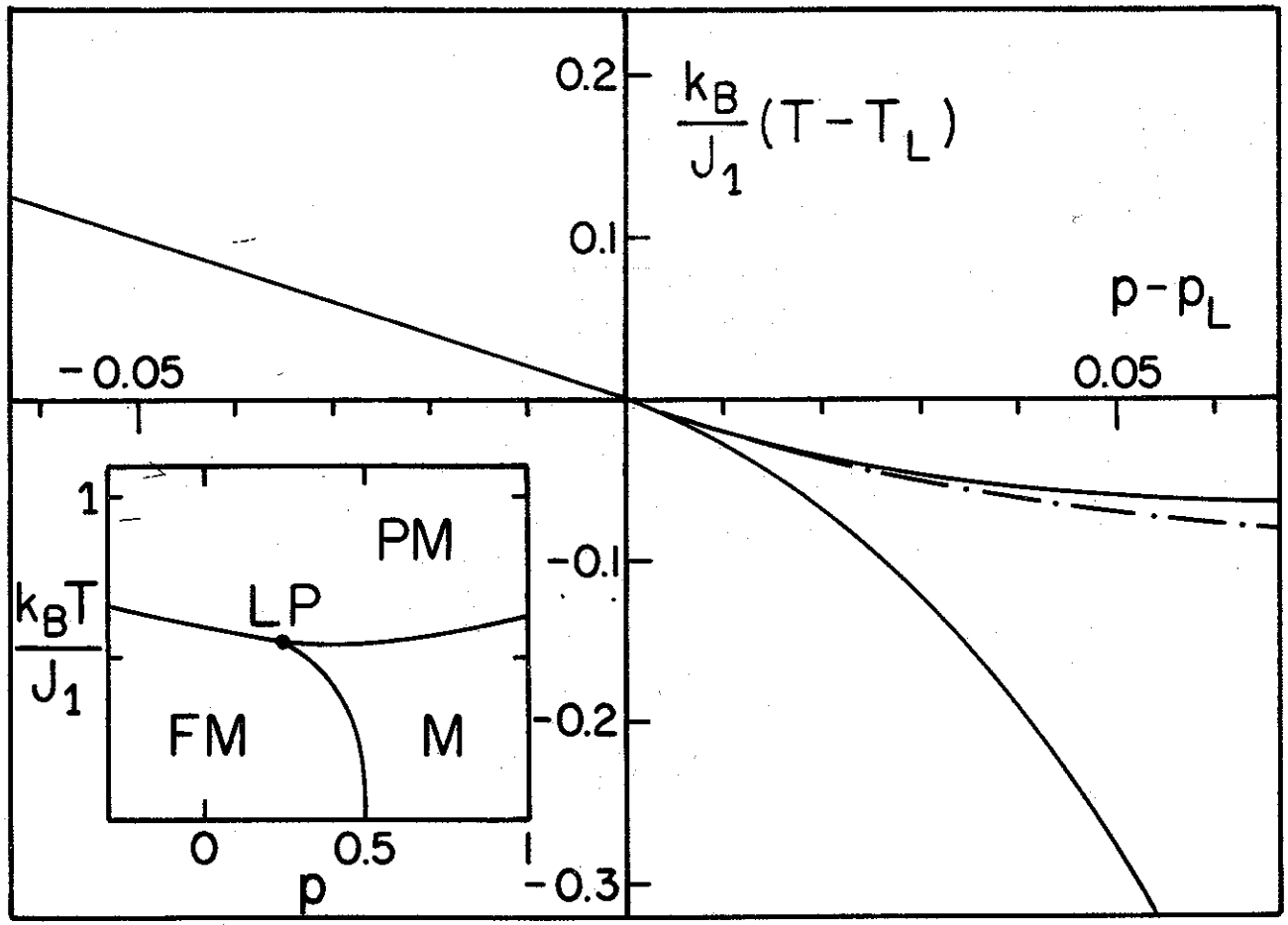
0.2
0.1
$\frac{k_B}{J_1}(T-T_L)$
$p-p_L$
-0.05
0.05
1
PM
$\frac{k_BT}{J_1}$
LP
FM
M
0
0.5
1
p
-0.1
-0.2
-0.3

FIG. 3

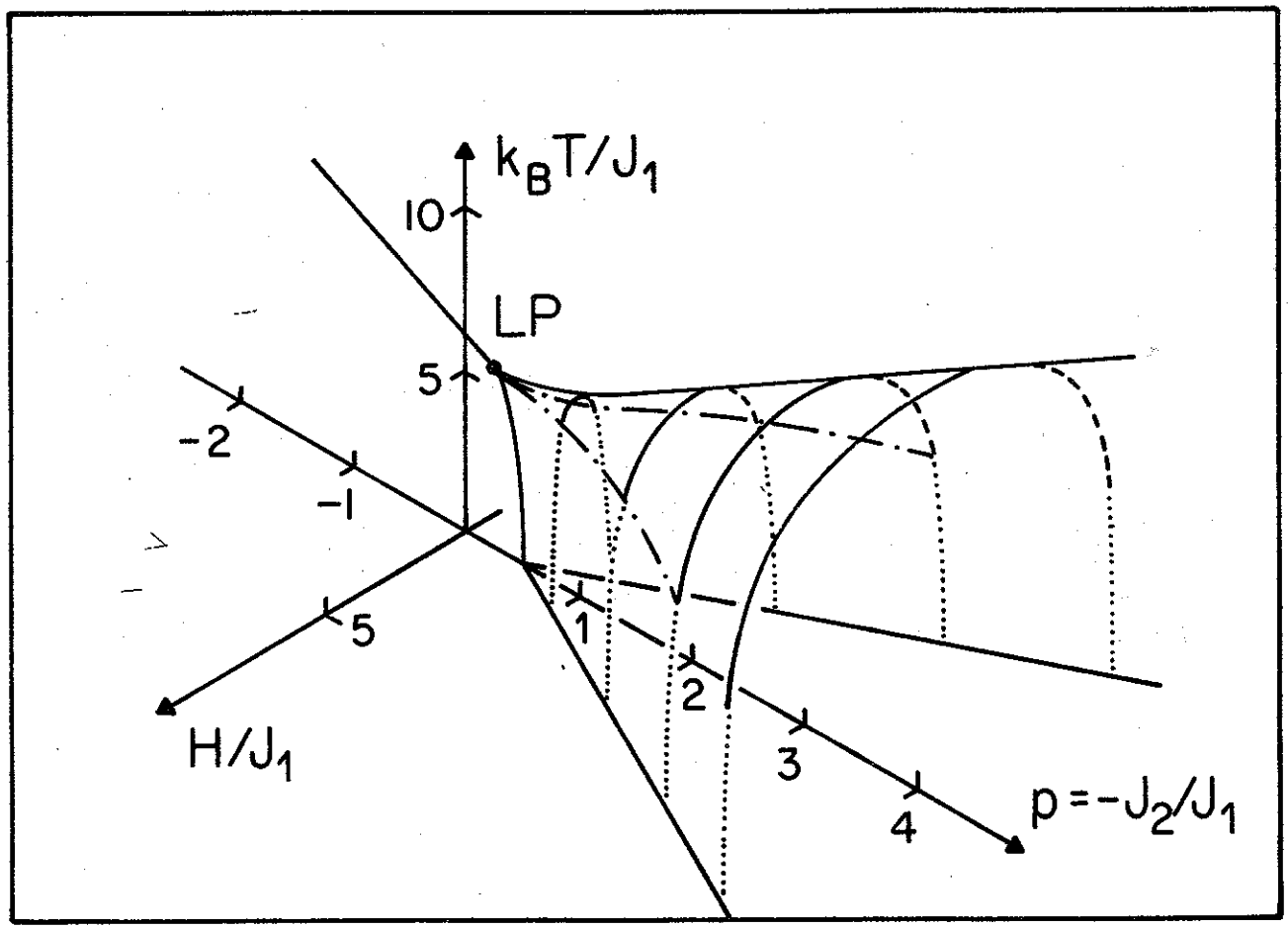

FIG. 4

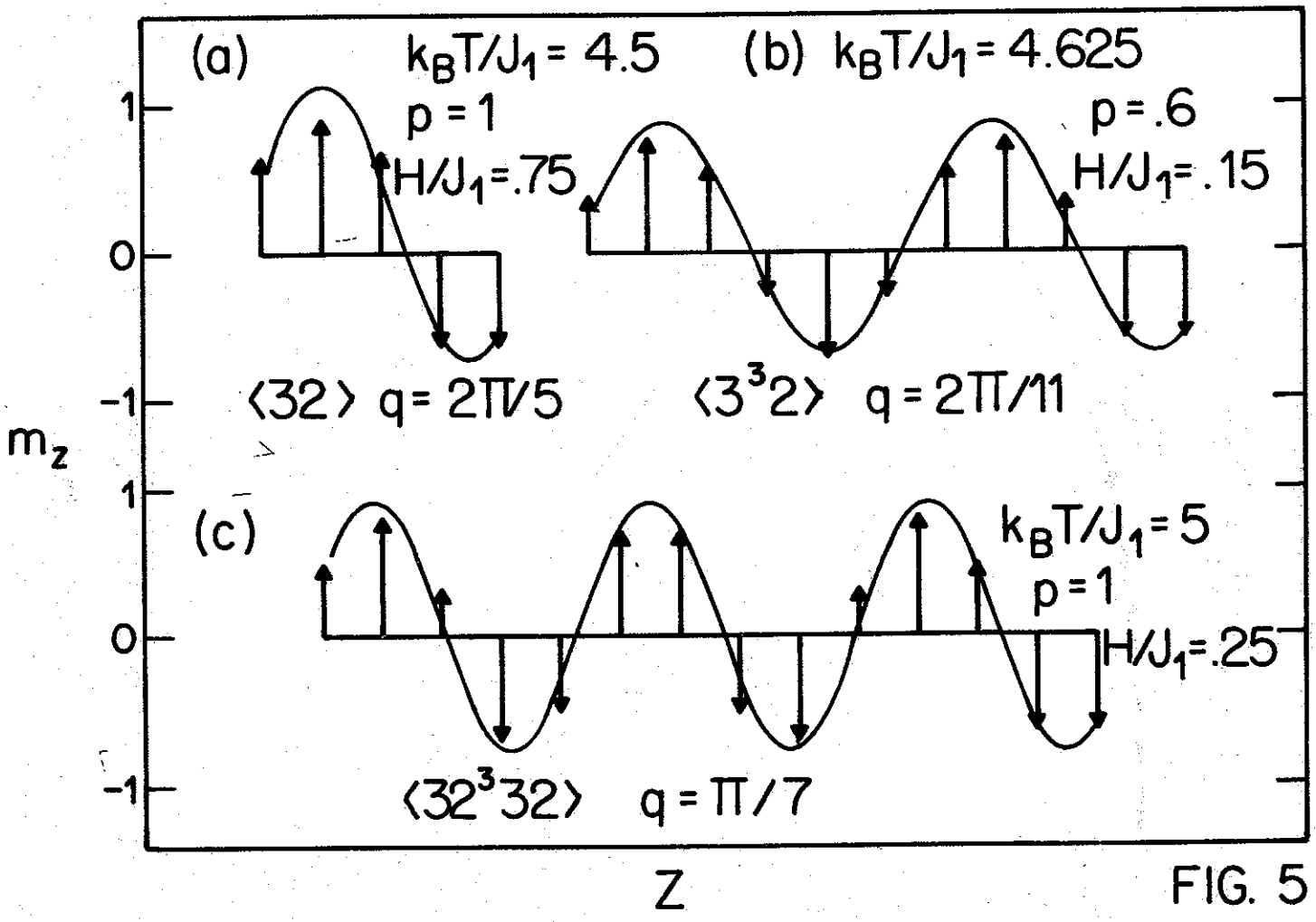
(a)
$k_BT/J_1 = 4.5$
p = 1
$H/J_1 = .75$
$\langle 32 \rangle$ q = 2π/5
(b) $k_BT/J_1 = 4.625$
p = .6
$H/J_1 = .15$
$\langle 3^3 2 \rangle$ q = 2π/11
(c)
$k_BT/J_1 = 5$
p = 1
$H/J_1 = .25$
$\langle 32^3 32 \rangle$ q = π/7
1
0
-1
1
0
-1
m_z
Z

FIG. 5

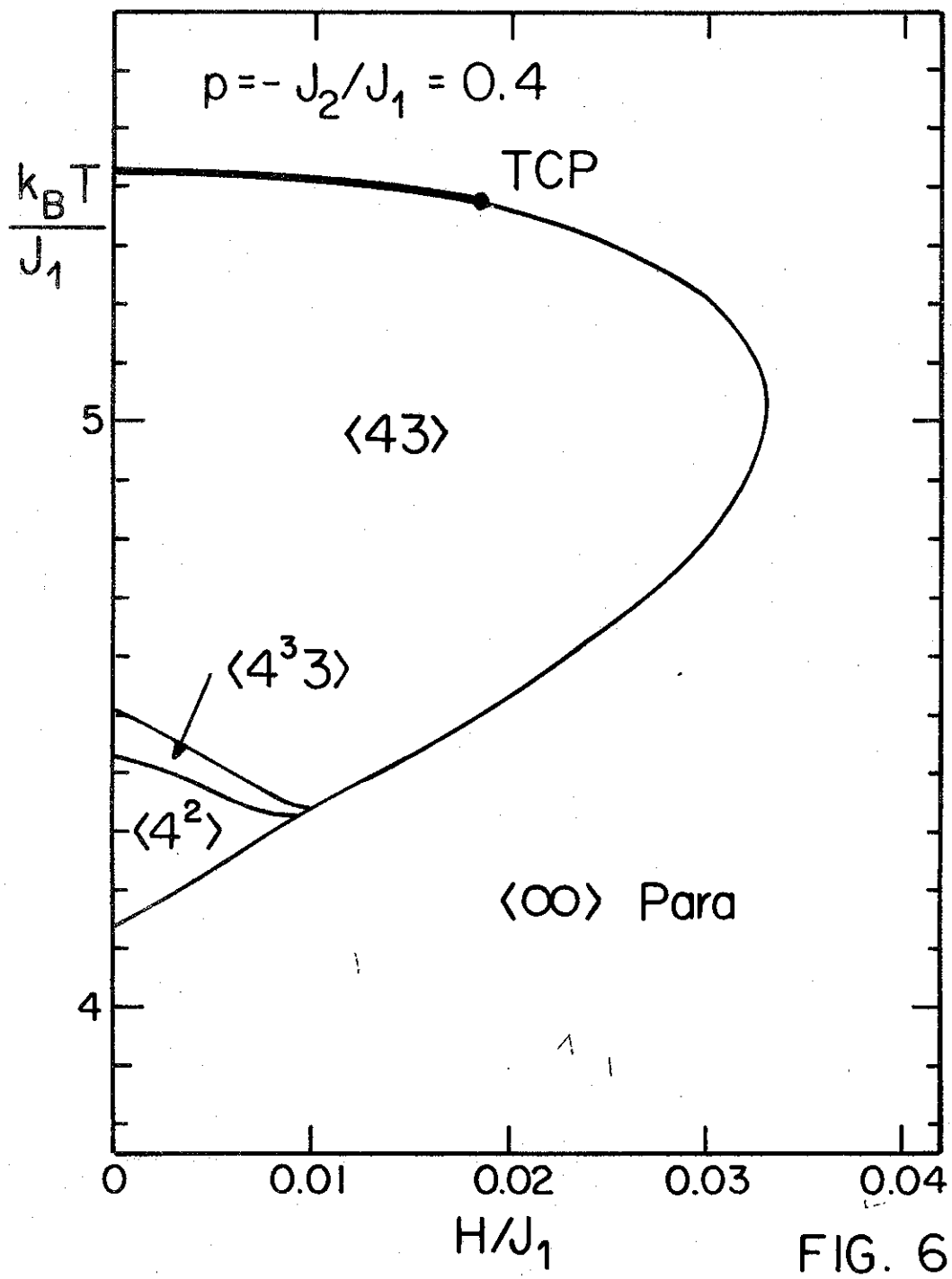

FIG. 6

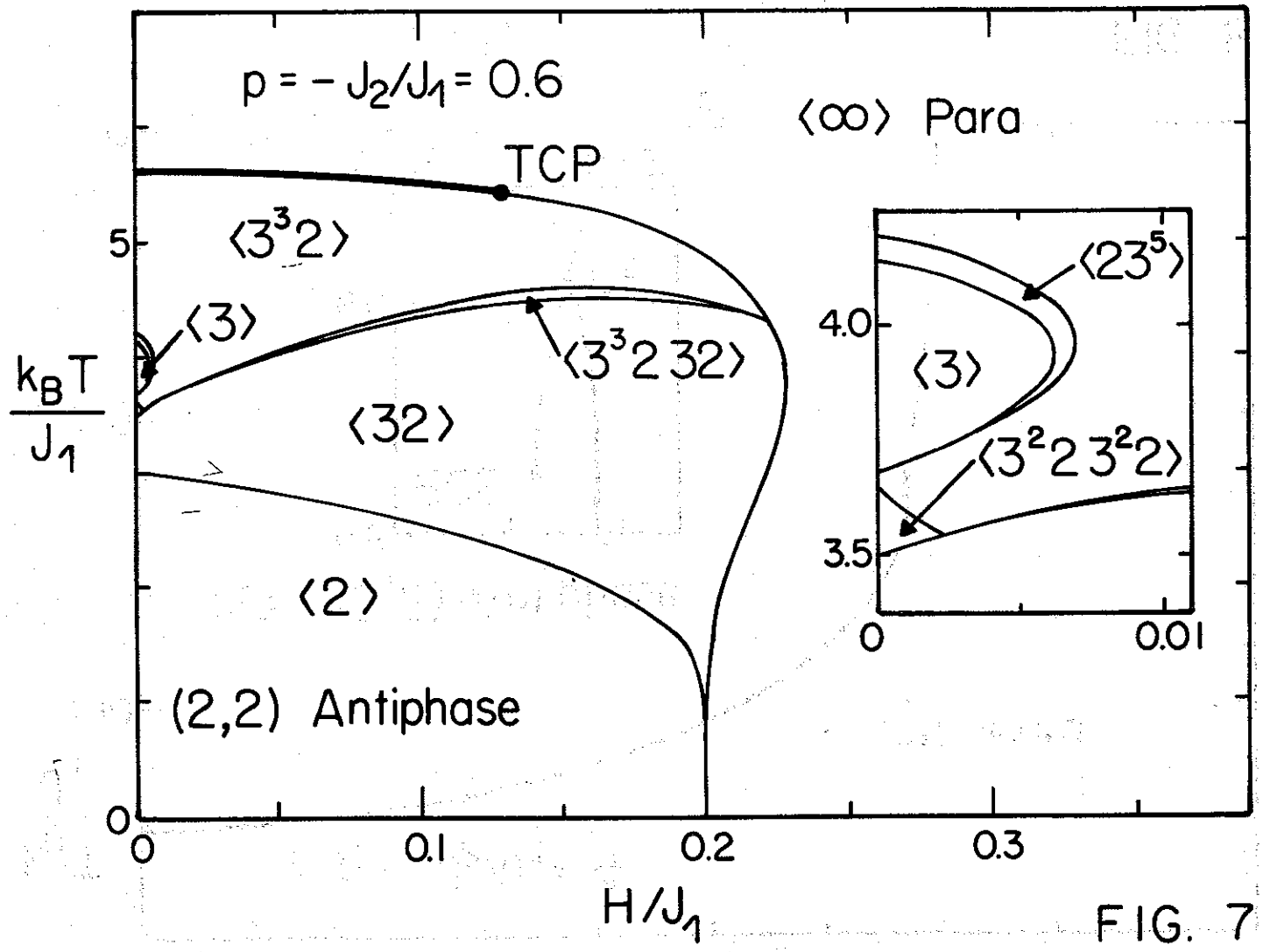
p = − J2/J1 = 0.6
⟨∞⟩ Para
TCP
⟨3³2⟩
⟨3⟩
⟨3³232⟩
⟨32⟩
⟨2⟩
(2,2) Antiphase
kBT/J1
H/J1
0
0.1
0.2
0.3
5
⟨23⁵⟩
4.0
⟨3⟩
⟨3²23²2⟩
3.5
0
0.01

FIG. 7

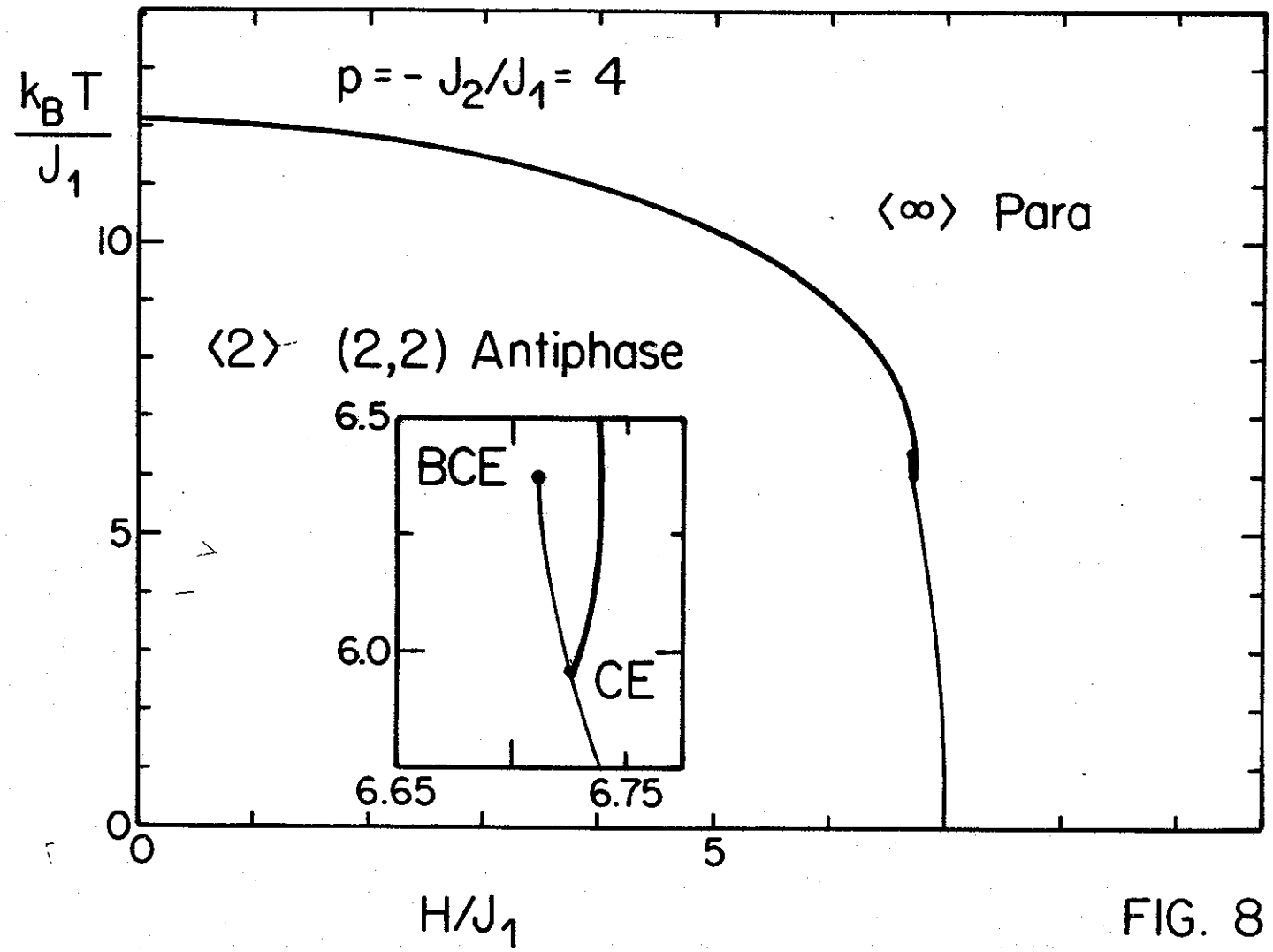
$k_B T / J_1$
$p = -J_2/J_1 = 4$
⟨∞⟩ Para
⟨2⟩ (2,2) Antiphase
BCE
CE
6.5
6.0
6.65
6.75
10
5
0
0
5
H/J_1

FIG. 8

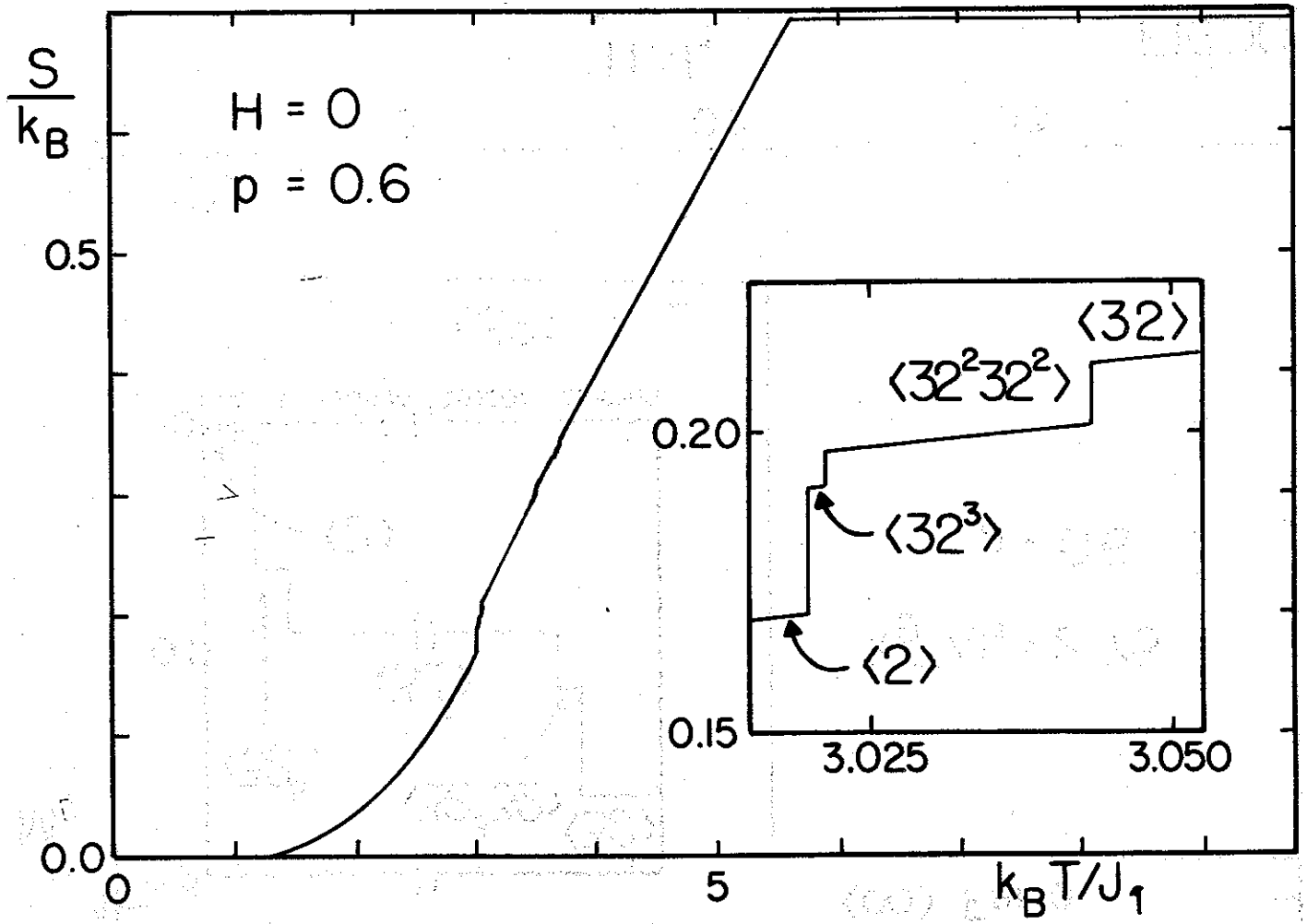

FIG. 9

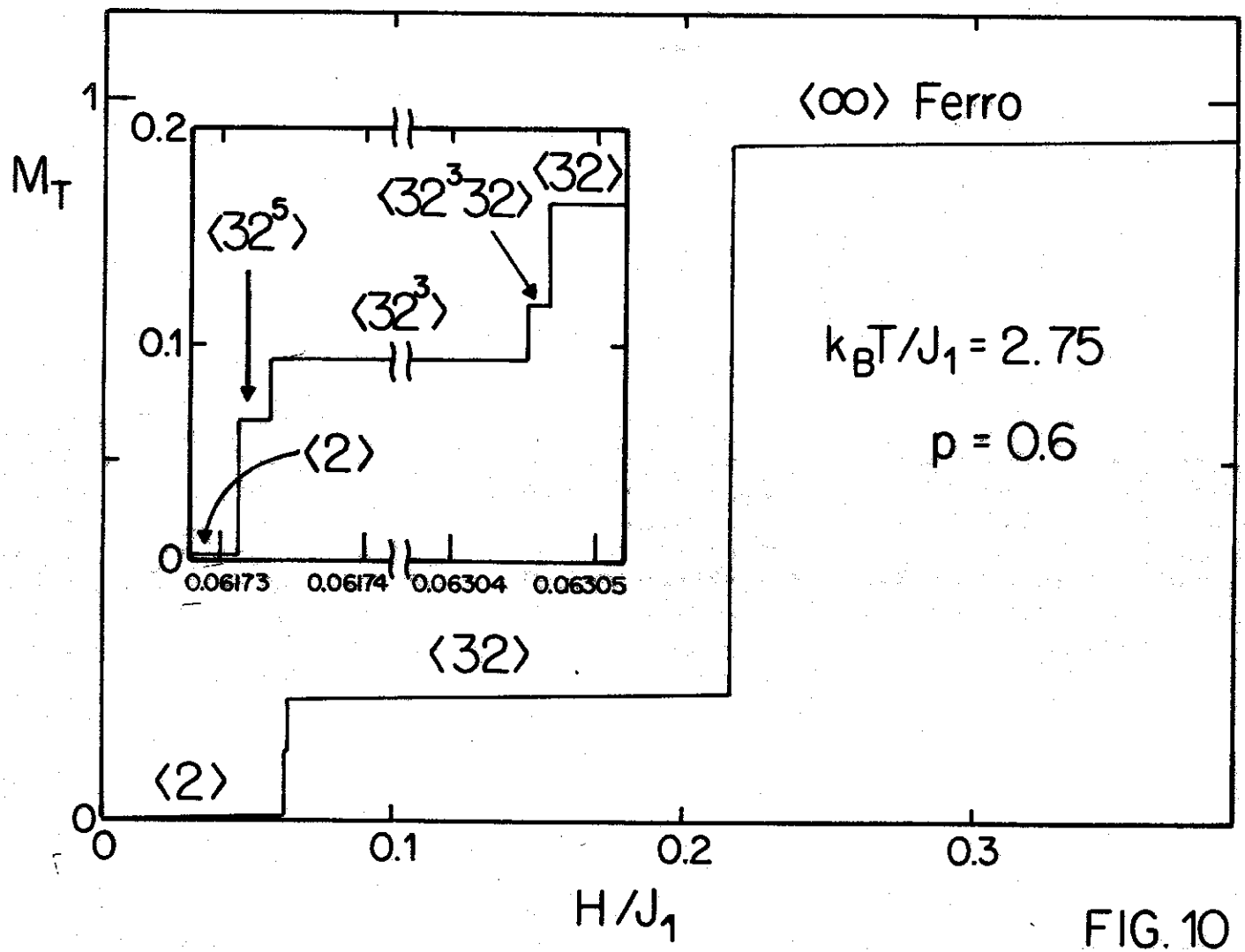
1
0.2
0.1
0
M_T
$\langle\infty\rangle$ Ferro
$\langle 32^5 \rangle$
$\langle 32^3 32 \rangle$
$\langle 32 \rangle$
$\langle 32^3 \rangle$
$\langle 2 \rangle$
0.06173
0.06174
0.06304
0.06305
$k_B T/J_1 = 2.75$
$p = 0.6$
$\langle 32 \rangle$
$\langle 2 \rangle$
0
0.1
0.2
0.3
H/J_1

FIG. 10

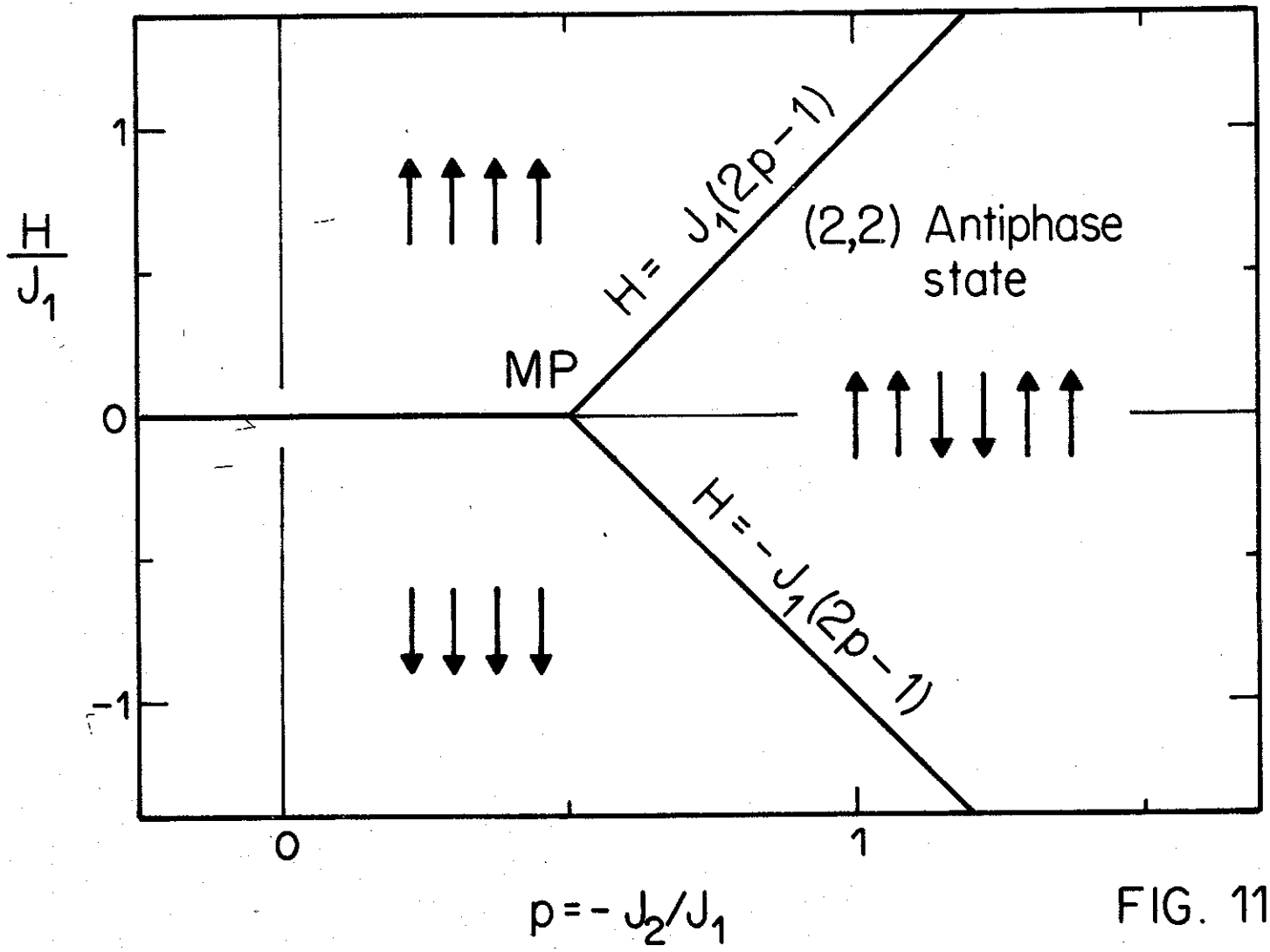

FIG. 11